Novel Perovskite Nanocrystal Synthesis Pathways to Obtain High Brightness Colour-Pure Emission: A Stepping Stone Towards High Efficiency LEDs

A Thesis

submitted to

Indian Institute of Science Education and Research Pune

in partial fulfillment of the requirements for the

BS-MS Dual Degree Programme

by

Mashale Sarang Siddharam

ID no: 20181190

INDIAN INSTITUTE OF SCIENCE EDUCATION AND RESEARCH PUNE

October, 2023

Supervisor: Dr. Aditya Sadhanala

Certificate

This is to certify that this dissertation entitled **Novel Perovskite Nanocrystal Synthesis Pathways to Obtain High Brightness Colour-Pure Emission: A Stepping Stone Towards High Efficiency LEDs** towards the partial fulfilment of the BS-MS dual degree programme at the Indian Institute of Science Education and Research Pune represents the work carried out by Mashale Sarang Siddharam at the Centre for Nanoscience and Engineering(CeNSE), Indian Institute of Science, Banglore under the supervision of Dr. Aditya Sadhanala, Centre for Nanoscience and Engineering(CeNSE), Indian Institute of Science Banglore during the academic year 2023.

Mashale Sarang Siddharam

Dr. Aditya Sadhanala

Thesis Advisory Committee:

Dr. Aditya Sadhanala

Prof. R. Vaidhyanathan

Declaration

I hereby declare that the matter embodied in the thesis entitled **Novel Perovskite Nanocrystal Synthesis Pathways to Obtain High Brightness Colour-Pure Emission: A Stepping Stone Towards High Efficiency LEDs** are the results of the work carried out by me under the supervision of Dr. Aditya Sadhanala at the Centre for Nanoscience and Engineering, Indian Institute of Science, Banglore and the same has not been submitted elsewhere for any other degree.

Mashale Sarang Siddharam

Dr. Aditya Sadhanala

This thesis is dedicated to anyone and everyone who believed in me.

Acknowledgements

Firstly and most importantly, I would like to express my sincere gratitude to my advisor Dr. Aditya Sadhanala for his patience, motivation, and continuous support throughout in my research. When I first joined our lab, I was a wide-eyed nervous guy, often feeling out of place, with little knowledge of how research is done on the academic level. I must thank him for the way he took me in his wings and taught me the nitty-gritty of doing research, from thinking, writing to the presentation part of it from the very grassroots level. Thank you so much, Sir, for your persistent belief in me, and truly I could not have imagined having a better advisor and mentor for my Master's Thesis.

Besides my advisor, I would also like to thank my Thesis Advisory Committee member: Dr. R. Vaidhyanathan for his encouragement and insightful comments. His comments helped me understand more deeply on the particular aspects of this project.

I would like to thank IISER Pune for providing all the facilities, from the library to the playgrounds, that made my stay pleasant here. I would like to acknowledge the Micro and Nano Characterization Facility(MNCF), CeNSE, IISc, Banglore, for providing access to the various characterization facilities.

I am grateful to my mentor, my Local Guru in Banglore, Jyoti Saxena, who trained me on the synthesis of Perovskite Nanocrystals and in device fabrication, it was a great experience setting up various experimental setups required for the characterization of the material and devices. Her constant support throughout my time in Banglore was crucial for me to quickly grabbing the skills required in this project.

I am also thankful to all the lab members of Advanced Opto and Nano Electronics(A-ONE) Lab for helping me throughout my project. I want to thank Dr Chaya for her help in the material characterization, Dr Sujay, Dr Sreekanth and Dr Laxman for their constant inputs on my work. Your suggestions always helped me to learn more about perovskites. I am also thankful to my fellow interns; Ankit, Nilima, Mayank, Divya and PhD Students; Avari, Poyoja, Anil, Vaibhavi,

Udit and Deepika, with you guys, the lab always felt like a second home.

My heartfelt thanks to each of my friends in IISER Pune for sharing all the joy, sorrow, happiness, and heartbreaks with me. I especially thank Arsh, Vedant, Monali, Rishabh, and Harshal; good times or bad times, you guys have always stood up for me. From last-moment anxious exam preparation to relaxed long night walks, from watching sports and movies together, my time in IISER, couldn't have been more enjoyable with you guys. I also want to thank Sanskar, Shikhar, Durvesh, Devarsh, Saikat for continuously supporting me.

From the depths of my heart, I also want to acknowledge my cricket teammates at IISER Pune, with whom I've shared countless moments of fun and camaraderie over the past five years. In particular, Team Alchemist has been instrumental in teaching me the importance of teamwork and believing in our collective strengths. My sincere thanks to Deb Bhaiya, Manjeet Bhaiya, Manzoor Bhaiya, Vijay Bhaiya, and all my senior teammates for their unwavering support. Playing cricket, especially alongside you all, has imparted invaluable life lessons, teaching me how to remain composed in high-pressure situations.

Beyond my time at IISER, I'd like to extend my gratitude to Pratik, Raghuveer, Sachin, Tanaya, Avanti, and Neha; your unwavering presence and support have meant the world to me. I'd also like to express my thanks to Ashutosh, Akshay, Harsh, and Jagadish for their contributions to making my time in Bangalore truly memorable.

Last but not the least, I sincerely acknowledge my family members for their endless encouragement, love, care and support in every stage of my life. Especially my parents, they have been constant pillars of strength for me, helping me unconditionally through many difficult moments in my life. So thank you and someday I hope to make you proud.

Sarang Mashale

Abstract

Lead halide perovskites (LHPs) constitute a promising semiconductor category for applications in photovoltaics (PV) and light-emitting diodes (LEDs) due to their versatile and readily adjustable optical properties. This thesis introduces an innovative approach to the Ligand Assisted Reprecipitation method employed for the synthesis of Perovskite Nanocrystals, utilizing a Methylamine/Acetonitrile compound solvent system. Additionally, a comprehensive overview of existing nanocrystal synthesis techniques, their advantages and limitations, is presented, along with a discussion of the characterization methods employed in their analysis. The low-temperature and easily scalable nature of this method offers an alternative to high-temperature perovskite nanocrystal synthesis. This work successfully demonstrates the synthesis of stable and highly luminescent Perovskite Red and Green Nanocrystals, elucidating their properties through optical spectroscopy and showcasing their applicability in Light Emitting devices. Furthermore, the thesis contributes a streamlined device architecture for a functional Red Perovskite LED. This readily scalable approach holds significant promise for industrial applications, and the thesis also outlines the future prospects for achieving operational Green and Blue Perovskite LEDs.

Figure 1: Green-Red Perovskite Nanocrystals under UV Illumination

Contents

List of Figures

Chapter 1

Introduction

1.1 Perovskites: Discovery and a brief history

How is a perovskite defined? Perovskite is a type of mineral that geologists originally discovered in the Ural Mountains in 1839. These minerals are common in the Earth's mantle, which is several hundred kilometres beneath our feet. Perovskites have, nevertheless, moved to the front of research efforts in science today. Any substance that adheres to a crystal structure like calcium titanate (CaTiO3) is regarded as a perovskite from a chemical perspective. As a result, there are many distinct types of perovskite materials, each of which has a wide range of intriguing and useful characteristics. For instance, whereas some cuprate perovskites, like YBa2Cu3O(7-x), show high-temperature superconductivity[31], barium titanate (BaTiO3) has a high dielectric constant and ferroelectricity[12]. Furthermore, some manganese oxide perovskites exhibit enormous magnetoresistance. However, over the past decade, the phrase "perovskite" has come to be associated with a specific subset: Metal Halide Perovskites. Over the past decade, there have been noteworthy advancements in our understanding of Metal Halide Perovskites, an emerging group of semiconductors that first emerged in the late 2000s[14]. These developments have unveiled compelling insights into their unique properties and potential applications. They have been widely investigated due to their promising photovoltaic and optoelectronic properties. Their ability to achieve g comparable performance to the expensive and high-performing semiconductor materials such as silicon, gallium arsenide, etc. through low-cost and highly scalable solution processing methods

have attracted researchers from all over the world.

1.2 Working of a Light Emitting Diode:

A conventional light-emitting diode (LED) comprises a P–N junction diode constructed from semiconducting materials. Electrons are injected from the n-side, while holes are injected from the p-side. Within the semiconductor, the recombination of electrons and holes leads to the emission of light.[3].

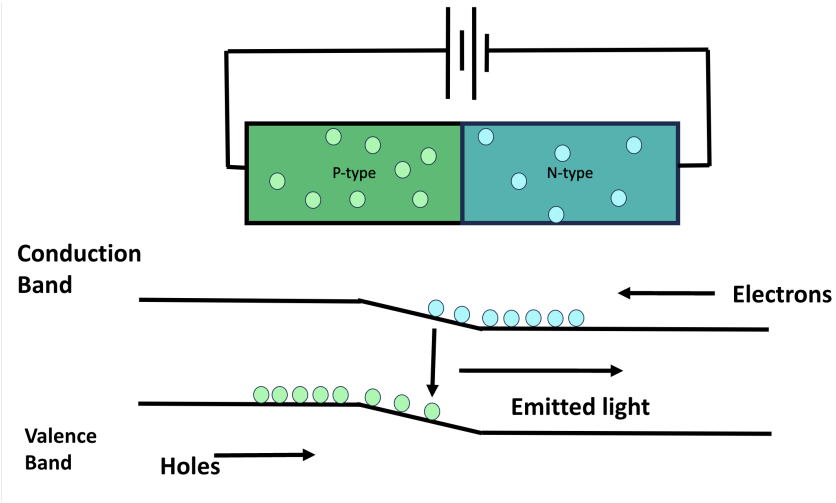

Figure 1.1: Schematic representation of a typical p-n junction LED

There are two types of electron and hole recombination: radiative and non-radiative. When an electron recombines with a hole in the valence band after moving from the conduction band, a photon is released. This process is known as radiative recombination. While complete elimination of non-radiative recombination may remain unattainable, its impact can be mitigated to enhance

the efficiency of Light Emitting Diodes (LEDs).

1.3 Perovskite Light Emitting Diodes: Status and Challenges:

In 1994, Era and colleagues achieved the construction of the inaugural organic-inorganic hybrid perovskite light-emitting diode (PeLED)[6]; however, its functionality was limited to extremely low temperatures, specifically within the range of liquid nitrogen temperatures. Based on their hypothesis, a hybrid material might incorporate advantageous properties of both organic and inorganic materials. In 2014, when the first research paper on a functioning PeLED operating at room temperature was published, PeLEDs attracted new attention[27].

Beginning in 2009, with the pioneering use of methylammonium lead iodide perovskite as an absorber material in solar cells, there has been a notable surge of research dedicated to the exploration of organic-inorganic hybrid perovskites[14]. Perovskite solar cell (PSC) research has significantly impacted Perovskite Light Emitting Diodes (PeLED) research because both technologies employ the same materials and have a similar device architecture. PeLEDs are part of a broader landscape of related technologies, including Organic Light-Emitting Diodes (OLEDs), Polymer Light-Emitting Diodes (PLEDs), and Quantum Dot Light-Emitting Diodes (QLEDs).

The evolution of Perovskite-based LEDs and current status can be understood by the following chart

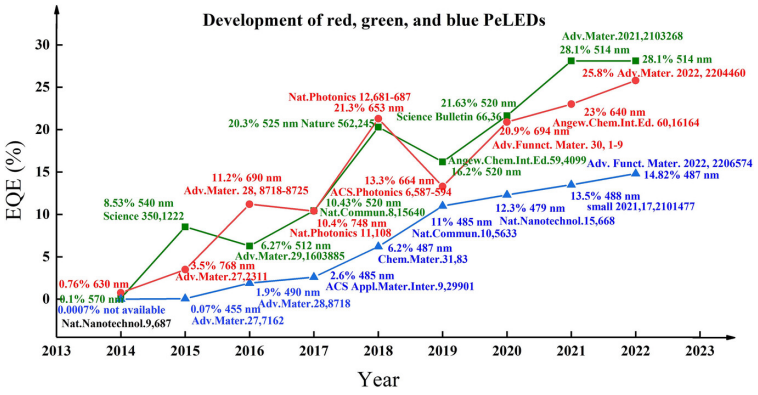

Figure 1.2: Evolution of External Quantum Efficiencies(EQEs) of Green, Red, and Blue emitting Perovskite-based LEDs.[33] **©Adapted from references with permission.**

1.4 Aim & Motivation of this thesis

The aim of the thesis is to develop an innovative approach to the synthesis of stable and highly luminescent Lead Halide Perovskite (LHP) nanocrystals. This is achieved by adapting the Ligand Assisted Reprecipitation method, utilizing a Methylamine/Acetonitrile compound solvent system, and demonstrating its potential as a low-temperature, easily scalable alternative to traditional high-temperature synthesis methods. The research also encompasses a comprehensive review of existing nanocrystal synthesis techniques, providing insights into their respective advantages and limitations. Moreover, the thesis aims to investigate the properties of the synthesized nanocrystals using optical spectroscopy and evaluate their suitability for use in Light Emitting devices. Additionally, it seeks to contribute a simplified device architecture for Red Perovskite LEDs, with the long-term goal of exploring avenues for the development of functional Green and Blue Perovskite LEDs, thereby addressing the prospects for industrial applications.

1.5 Outline of this Thesis

The basic background on discovery and history of Perovskites followed by working principle and status of Perovskite based LEDs is presented in this chapter (**Chapter 1: Introduction**). This is followed by various fundamental properties which makes them promising candidate for Light Emitting applications being discussed in the **Chapter 2: Fundamentals**. **Chapter 3:Characterizaton Techniques** talks about the characterization techniques used by us for characterizing the Perovskite nanocrystals, this chapter briefly talks about the optical absorption and emission spectroscopy, X-Ray Diffraction and a highly sensitive method of direct measurement of PLQY used by us. **Chapter 4: Methodlogy** describes the different methods of synthesizing perovskite nanocrystals followed by synthesis of Red Emitting Perovskite nanocrystals in **Chapter 5: Red Emitting Perovskite Nanocrystals** and our efforts towards Green-Blue Perovskite Nanocrystals being discussed in **Chapter 6:Towards Green-Blue Nanocrystals**. A brief discussion on Perovskite LEDs is presented in **Chapter 7: Device Fabrication** and the thesis is concluded by the **Challenges and limitations** of this work.

Chapter 2

Fundamentals

The basic fundamental properties of perovskites which makes them excellent materials for opto-electronic device applications, will be briefly discussed in this chapter.

2.1 Structure

The term 'Perovskite' finds its origins in the mineral Calcium titanate ($CaTiO_3$), initially discovered in the Ural Mountains in 1839 and named after the mineralogist Lev Perovski. This mineral marked the inception of the structural type now commonly associated with the Perovskite class of materials. Metal Halide Perovskites adhere to the ABX3 stoichiometry, where 'A' represents a monovalent cation, typically Methyl Ammonium, Formamidinium, or Cesium; 'B' denotes a divalent cation, such as Lead or Tin; and 'X' signifies halide atoms (e.g., Cl, Br, I). Within the crystal lattice, a network of BX_6 Octahedra is present, with the A-site occupying body-centred positions. The attainment of a perfectly cubic perovskite structure is exceedingly rare, as most perovskites exhibit either orthorhombic or distorted tetragonal structures due to the arrangement of constituent atoms within the crystal lattice.

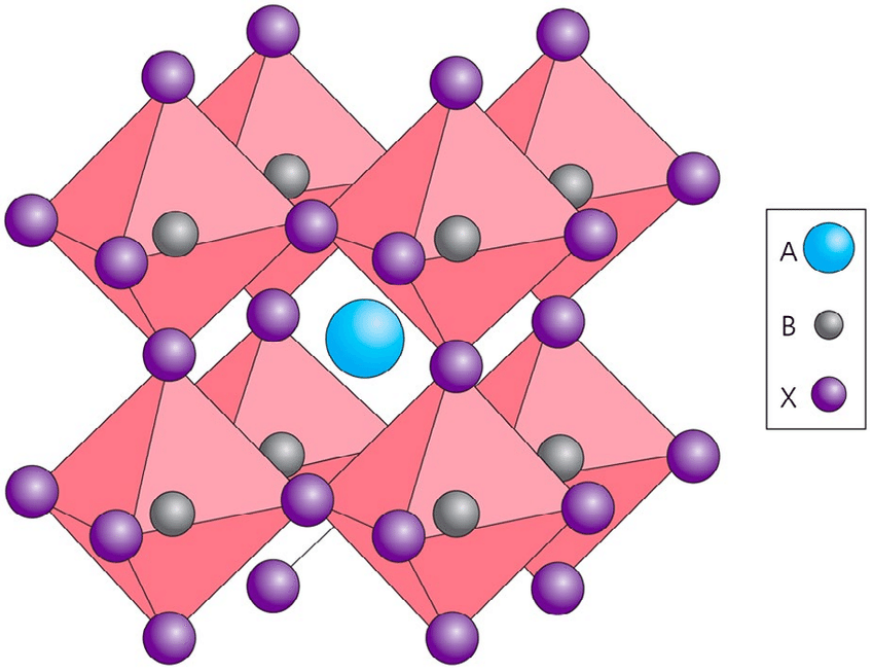

Figure 2.1: Typical structure of ABX_3 Perovskite **©Adapted from refrences**[9]

2.1.1 Tolerance Factor:

There are numerous possible perovskite compositions which still need to be investigated. Goldschmidt tolerance factor[17] serves as a guiding metric for ascertaining the potential of a given chemical composition to yield a stable perovskite structure.

$$t = \frac{r_A + r_B}{\sqrt{2}\,(r_B + r_X)}$$

A solid-state crystal structure is expected when the value of 't' is between 0.8 and 1. Having a 't' value more than 1 restricts the formation of perovskite structure while a value less than 0.8 results in non-perovskite structure.

2.2 Defect tolerance:

Point defects are present in all crystalline materials. These structural defects can take one of three typical forms: interstitials, where atoms occupy sites in the lattice that ought to be vacant; antisites, where an atom occupies a site other than the one it is supposed to; or vacancies, simply sites with missing atoms. Depending on the material's structure, different defects will have different relative production energies. The extent to which the creation of energetically feasible defects impacts a material's electrical characteristics is referred to as its defect tolerance. Lead halide perovskites are typically thought to be quite forgiving of flaws.

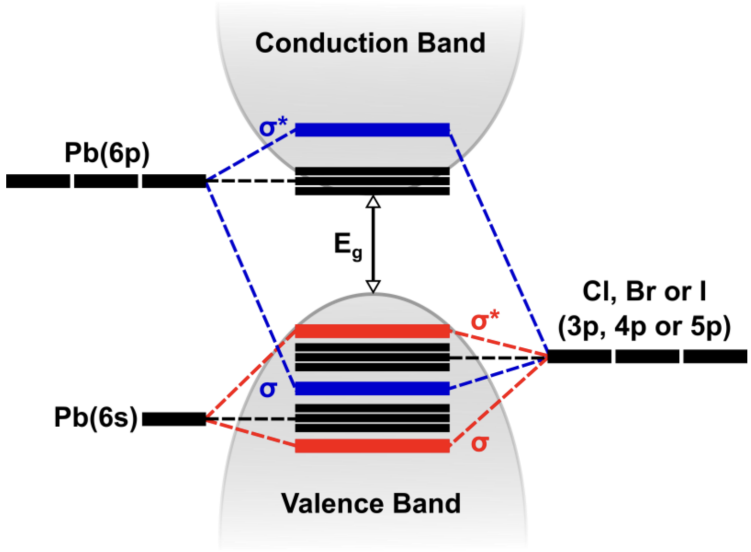

Figure 2.2: Band structure of $APbX_3$ Perovskites. **©Adapted from references**[4, 15]

The remarkable defect tolerance exhibited in perovskite structures can be attributed to the benign nature of thermodynamically favourable trap states. Within these structures, a substantial prevalence of X-site vacancies is observed, while the emergence of interstitial, antisite, and Pb2+ vacancies is exceedingly improbable. Notably, these halide vacancies exclusively manifest as in-band or shallow trap states, thereby preserving outstanding optoelectronic properties even in the

presence of defect densities that would render alternative materials nonviable. Their defect tolerance supports some of the most appealing properties of lead halide perovskites[1, 13]. Perovskite materials can be prepared using laboratory-grade solvents in ambient circumstances because the induced defects little affect their properties. Due to their particular suitability for solution processing, there is a significant chance that large-scale, high-throughput industrial procedures will be practical and affordable.

2.3 Bandgap tunability

Perovskite materials possess a direct bandgap characteristic, resulting in the emission of nearly monochromatic light when subjected to optical excitation, as in photoluminescence, or electrical excitation, as in electroluminescence. The emitted colour is contingent upon the bandgap energies inherent to the materials. Notably, the wavelength of this emission exhibits a direct correlation with the bandgap of the light-emitting constituent in Light Emitting Diodes (LEDs). Strong compositional lability can be observed by selecting at least three different cations and three different anions and combining them in the required ratios. This is a beneficial property because the composition significantly impacts the optoelectronic capabilities of perovskites. A semiconductor's bandgap is more or less linearly related to the lattice characteristics. The interatomic distance reduces as the lattice parameter shrinks, increasing the bandgap and valence electron binding energy. As the figure shows, the valence band and conduction band of an $APbX_3$ Perovskite is formed by the interaction of atomic orbitals of the Lead atoms and halide atoms. The valence band maximum (VBM) is the result of antibonding hybrid states between a significant amount of p-orbitals of X anions and a minor portion of s-orbitals of Lead (Pb) cation. The hybridization of 6p-orbitals of Lead (Pb) cations creates the conduction band minimum (CBM). As a result, there are substantial variations among distinct halides in the energy of the valence band maximum and, to a lesser extent, the conduction band minimum. This immediately changes the perovskite's bandgap,

a fundamental optoelectronic property that determines the material's light absorption and emission profile. Fig shows the bandgap tuning of $CsPbX_3$ nanocrystals over the whole visible range reported by Protesescu et al[23].

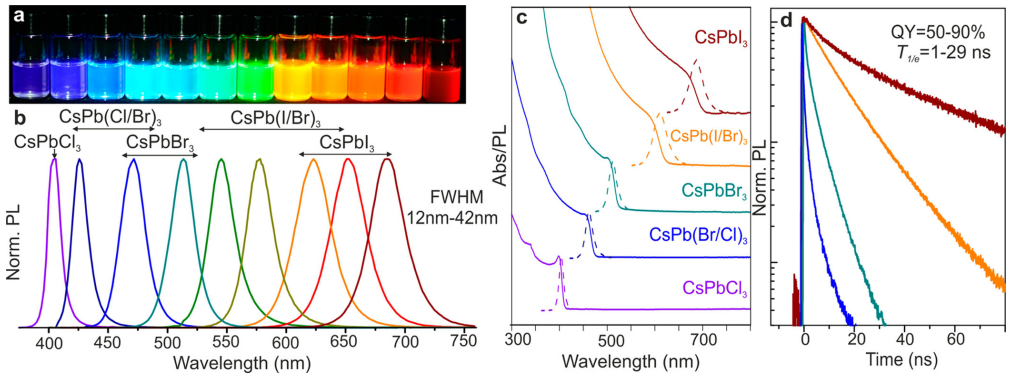

Figure 2.3: Bandgap tuning of CsPbX3 nanocrystals. a) CsPbX3 nanocrystals colloidal dispersions under UV light illumination, b) Photoluminescence spectra of CsPbX3 samples.[23] **©Adapted from ref. and Reprinted with permission.**

2.4 Nanocrystals

In the last decade, Lead Halide Perovskite Nanocrystals have surfaced as remarkable materials with immense potential for applications in light emission. This potential arises from the capacity to enhance radiative recombination through the deliberate manipulation of crystal size[2, 26]. In other words, an exciton pair of electrons and holes confined in a smaller volume will have a high chance of combining with each other. Therefore, radiative recombination will occur more frequently in smaller crystals, this phenomenon is known as 'Spatial Confinement' and it has effects

to any crystal sizes. Nanocrystals benefit from additional phenomena that are peculiar to smaller crystals, where the electrical structure changes significantly from that of the bulk. The electrical structure of a crystal changes from a delocalized quasi-continuous band to a collection of discrete, distinct states when the number of MOs within the crystal diminishes. This is known as 'Quantum Confinement.'

2.5 Photoluminescence Quantum Yield:

The percentage of total photons emitted per photons absorbed is the photoluminescence quantum yield (PLQY), a measure of how effectively a luminous material emits light. It is described as the ratio of radiative recombination to all other processes, such as photoluminescence's non-radiative transitions. The excitation intensity has a major effect on the PLQY value. Monomolecular recombination of traps limits the PLQY at low charge carrier densities. When there is a high charge carrier density, the traps are mostly filled and bimolecular recombination of free carries takes over, which causes PLQY to rise until Auger recombination is in effect. The effectiveness of the active material used to produce electroluminescence has a direct bearing on the efficiency of LEDs. As a result, there is a clear positive link between device performance and PLQY, and increasing this number boosts the effectiveness of the ensuing solid-state devices.

$$\Phi = \frac{\text{Photons emitted}}{\text{Photons absorbed}} \tag{2.1}$$

2.6 Color Purity and narrow spectral bandwidth:

A key criterion for evaluating display quality is colour purity. Perovskites' luminescence spectra are typically narrow, thus rendering them advantageous for high-end display applications[8]. This remains true regardless of how they are prepared and the size of the grains. In contrast to quan-

tum dot LEDs, perovskite LEDs have a significant advantage since quantum dots need a restricted particle size distribution to create a narrow spectral width. In contrast to perovskites, which don't require specialised processing methods to regulate their grain size distribution, quantum dots require a restricted particle size distribution, which unavoidably raises the complexity and cost of creation.

Perovskites have a number of favourable characteristics that make them promising photovoltaic absorbers as well as electroluminescent materials. A considerable fraction of carriers can be removed from the electrodes (as in a solar cell) or recombined radiatively (as in an LED) thanks to low charge trap density and the high tolerance of the electronic structure for these traps. A substantial photon absorption coefficient[14], long and balanced charge carrier diffusion lengths[30, 32] and high charge carrier mobility[25, 30] contribute to effective photon collection and emission. A low exciton binding energy, however, prevents radiative recombination in 3D perovskites.

Chapter 3

Characterization Techniques:

The techniques used in this thesis to characterize the Perovskite nanocrystals and their devices will be briefly explained in this chapter.

3.1 Optical Absorption and Photoluminescence spectroscopy

In the realm of semiconductor and electronic system research, optical absorption and photoluminescence spectroscopy represent indispensable, non-intrusive methodologies. These techniques play a pivotal role in elucidating the fundamental properties of semiconductors, thereby contributing to the advancement of photovoltaic technology. Specifically, the precise determination of a semiconductor layer's bandgap and the quantification of absorbed light within a solar cell device are critical endeavours. These measurements serve as foundational steps towards establishing the theoretical upper limits for power conversion efficiency and photovoltaic parameters in future solar cell technologies.

Furthermore, the analysis of luminescent properties in semiconductors holds paramount importance in comprehending and mitigating losses encountered in optoelectronic devices. It is essential to note that the optical bandgap, a fundamental parameter governing a semiconductor's photonic properties, is linked to the theoretical limits of various optoelectronic device parameters. This critical parameter is determined by the absorption characteristics of the photo-absorber semiconductor, thus underscoring its significance in the context of semiconductor applications within optoelectronic systems.

Of interest is the unique attribute of metal-halide perovskite semiconductors, characterized by a direct bandgap. This feature enables thin films of perovskite materials to efficiently absorb incident light, in stark contrast to indirect bandgap-based semiconductors like silicon, which necessitate larger film thicknesses to achieve comparable light absorption efficiencies. This distinction underscores the promise of metal-halide perovskites as leading contenders for the next generation of optoelectronic devices, owing to their exceptional light-absorption characteristics.

3.2 UV-Vis Absorption Spectroscopy:

Absorption spectroscopy in the Ultraviolet-Visible-Near Infrared region is termed UV-Vis-NIR Spectroscopy. Qualitative insights into material properties can be garnered through the absorption of ultraviolet (UV) and visible light, a foundational aspect of optical spectroscopy. Photoluminescence (PL) and electroluminescence (EL) peaks exhibit a discernible interrelation with the material's absorbance characteristics. Notably, in proximity to the PL peak, the absorbance spectra manifest a distinctive feature namely, a pronounced, abrupt onset with the capacity to capture and attenuate emissions at shorter wavelengths. This observed correlation underscores the utility of optical absorption techniques in elucidating the optoelectronic behavior of materials, particularly in the context of their emission characteristics. The Absorption is given by the Beer-Lambert law:

$$A = \log_{10}\left(\frac{I}{I_0}\right) \tag{3.1}$$

The absorbance spectrum of a semiconductor provides crucial insights into its light-absorption behavior across varying wavelengths. In proximity to the photoluminescence (PL) peak, a distinctive feature , characterized by a sharp and pronounced edge, emerges within the absorbance

spectrum. This phenomenon is attributed to the semiconductor's capacity to absorb incident light at wavelengths shorter than the energy of its bandgap. This efficient absorption occurs due to the surplus energy carried by the absorbed photons, enabling the excitation of electrons from the valence band to the conduction band.

In the broader context, the absorption of ultraviolet (UV) and visible light constitutes a valuable avenue for acquiring comprehensive information concerning the optical properties of semiconductor materials. The interrelation observed among the PL, electroluminescence (EL), and absorbance peaks serves as a powerful tool for elucidating critical aspects of semiconductor behavior. This includes the precise determination of the semiconductor's bandgap energy and a deeper comprehension of the recombination processes governing its optoelectronic behavior.

3.3 Photoluminescence Spectroscopy:

In PL spectroscopy, the emission spectra is captured after the film is stimulated by photons that are typically more energetic than the band gap. The emission characteristics inherent to perovskite absorbers offer compelling insights into the exceptional performance observed in perovskite-based optoelectronic devices. These versatile perovskite semiconductors exhibit broad light absorption profiles that correspond to their specific bandgap energies. This absorption process engenders the generation of charge carriers within the material, which subsequently undergo relaxation towards the energy minima of the conduction band and valence band. These charge carriers then partake in radiative recombination processes, resulting in robust emission characteristics.

For instance, perovskites display an impressively wide spectral responsiveness, signifying their ability to absorb photons spanning diverse energy levels. This absorption mechanism generates a predominance of free charge carriers, which recombine near the uppermost valence band and the

lowermost conduction band levels. Importantly, this band-to-band relaxation process is inherently radiative in nature, culminating in the emission of intense and narrowly distributed light. The remarkable attribute of perovskites, characterized by their intense and narrow emission, positions them as highly prospective candidates for light-emitting diodes (LEDs). Within the photoluminescence (PL) spectrum lies a wealth of crucial information regarding a material's attributes, including the band edge, the presence of excitonic peaks, the identification of trap states, and the degree of electron-phonon interactions. Furthermore, by examining the temperature-dependent PL spectrum, it becomes feasible to make estimations of the exciton binding energy.

In our PL measurements, an in-house-built system was used, where the perovskite film was excited with a 405nm Laser source, and the QE Pro High-Performance recorded the subsequent emission spectrum Spectrometer through an optic fibre.

3.4 X-Ray Diffraction:

Perovskite materials are amenable to investigation through X-ray diffraction (XRD) techniques, a nondestructive method frequently employed for their characterization. XRD, in its application, can involve the utilization of single crystals, thin films, or powdered samples. This method offers a wealth of valuable insights into perovskite materials, with several pertinent examples presented herein. XRD is based on Bragg's law,

$$n\lambda = 2d \sin\theta$$

In XRD analysis, the material's characterization is achieved through the diffraction of X-ray

radiation as it interacts with the sample. The comparison of acquired XRD data with established diffraction patterns from databases, such as those provided by the International Centre for Diffraction Data, facilitates the determination of both composition and structural attributes of the examined materials. Furthermore, XRD serves as a valuable tool for assessing the purity of perovskite samples. In instances where no impurity peaks are detected, it is reasonable to infer that impurities are present at levels below 0.5 weight percent or are undetectable based on the diffractometer's sensitivity threshold. Additionally, XRD enables the detection of distinct phases within the same material, further enhancing its utility in perovskite characterization.

Overall, XRD is a powerful tool for characterizing perovskite materials. It is non-destructive, versatile, and can provide detailed information about the composition, structure, and purity of perovskites.

3.5 Photoluminescence Quantum Yield (PLQY):

The assessment of photoluminescence quantum yield (PLQY) serves as a fundamental metric in the evaluation of luminescent materials. Beyond its role as an essential criterion in material characterization, the ratio of emitted photons to absorbed photons is pivotal for comprehensive investigations of luminescent systems and phenomena. Over the years, numerous methodologies for PLQY determination have been documented in the literature. When equipped with the appropriate instrumentation, it is feasible to directly measure absolute PLQY values, albeit with a high degree of sensitivity and precision, contingent upon accurate photon counting.

Commonly adopted approaches to calculating PLQY include a comparative method, often employed for solutions, in which the luminescence of the target molecule is juxtaposed against that of a known standard [18, 29]. Conversely, a distinct approach involves the direct quantification of PLQY through the direct counting of emitted and absorbed photons. The pioneering work by de Mello and colleagues in 1997[5], building upon ideas they had previously reported in 1995[10],

introduced this method. Presently, this method is widely adopted and boasts over 1100 citations, primarily in the context of solutions[7]. The direct determination of PLQY offers several advantages over the comparative method.

The precise determination of Photoluminescence Quantum Yield (PLQY) necessitates a meticulous three-step methodology. Initially, the intensity of the incident laser is measured with an empty integrating sphere as the baseline reference. Subsequently, the sample is introduced into the sphere, and the laser beam is directed at the interior surface of the sphere's wall, facilitating the recording of the emission spectrum. This emission spectrum is generated through the interaction between incident laser photons and the sample, as light is absorbed and re-emitted. This process is instrumental in addressing potential re-absorption phenomena, particularly when the absorption and emission spectra substantially overlap. In the third and final step, the laser beam is meticulously focused on the sample, enabling the capture of its emission spectrum. An essential consideration during this phase is the precise orientation of the sample to ensure that incident laser light reflects off the sample's surface toward the spherical wall, rather than escaping through the laser entrance aperture. Subsequently, the PLQE is computed through the judicious amalgamation of data acquired from these three sequential steps. This rigorous procedure establishes a robust and reliable framework for the quantification of Photoluminescence Quantum Yield, thereby enhancing the precision and validity of photoluminescence research and its myriad applications.

These three sequential measurements, designated as A (measurement with an empty sphere), B (indirect sample illumination), and C (direct sample illumination), as per the original terminology, are integral to this process. It is imperative to note that the transformation of measured intensity data into photon counts is contingent upon the specific detector employed. Each spectrum captured during these measurements comprises two distinct components: the excitation (X) and emission (E) spectra. By independently integrating these components, it becomes feasible to calculate the PLQY (Φ) and Absorbance (A). It is calculated by using following equations[7].

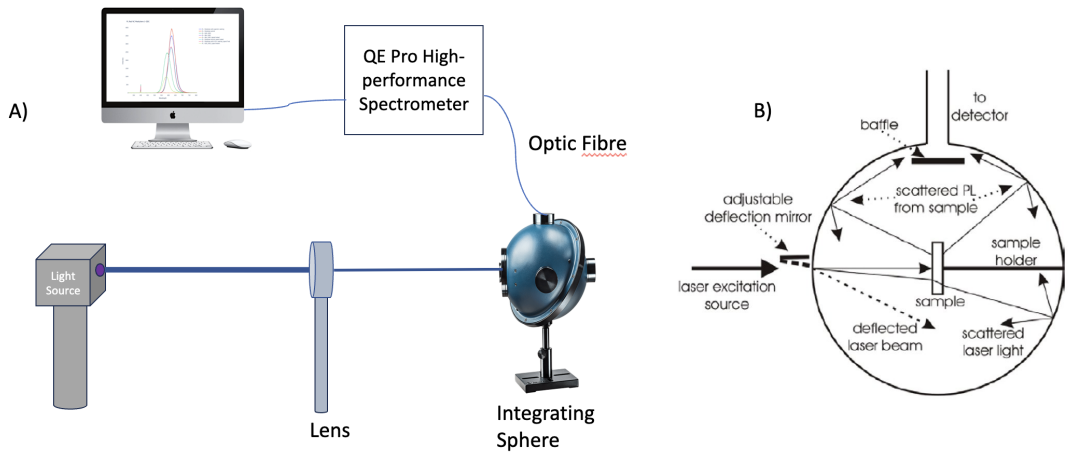

Figure 3.1: A)Schematic representation of our in-house built PLQY setup. B)Illustration of experimental measurement of PLQY inside the Integrating sphere[5]**©Adapted from references**

$$A = \left(1 - \frac{X_{\mathrm{C}}}{X_{\mathrm{B}}}\right) \tag{3.2}$$

$$PLQY, \Phi = \frac{(E_{\mathrm{C}} - (1-A)\,E_{\mathrm{B}})}{A.X_{\mathrm{A}}} \tag{3.3}$$

This methodological framework ensures the rigorous and precise assessment of PLQY, thereby contributing to the advancement of research in photoluminescent materials and their applications.

Chapter 4

Methodology

Confined semiconductor nanocrystals are particularly appealing for light-emitting applications because to the enhanced luminosity they provide. The enormous surface area of bare nanocrystals makes them thermodynamically unstable. In order to lower the surface energy of the nanocrystals and prevent the agglomeration of nearby nanocrystals into a single bigger crystal, surfactants must be applied to their surfaces. A surfactant is an amphiphilic molecule with a long non-polar alkyl "tail" and a short polar "head" group. The terminology used in this work will be ligands, which is the term used to describe surfactants that bind to nanocrystals. The organic ligands' properties greatly influence numerous characteristics of the resulting electroluminescent devices and perovskite nanocrystal inks. The effectiveness and stability of surface defect passivation depend greatly on the nature of the interaction between the ligand binding group and the nanocrystal surface[19, 24]. When deposited as thin films for electrical devices, the ligand tail's length, bulk, and branching significantly impact the conductivity and colloidal stability of the nanocrystals[22]. Additionally, because colloidal synthesis is a one-pot process, the effects of purifying procedures that are required to get rid of excesses and reaction byproducts must also be taken into account[16, ?]. Beyond the characteristics of certain ligands, the synthesis process used affects the perovskite nanocrystals' commercial potential. Mostly, airless, high-temperature "hot-injection" syntheses are used, which are difficult to scale up. Synthesis processes carried out at room temperature, particularly those without environmental restrictions, are significantly more appealing economically. The various methods used for the preparation of the colloidal Perovskite Nanocrys-

tals will be briefly discussed in this chapter, followed by a description of the setup and process used by us.

4.1 Synthesis of Perovskite Nanocrystals:

The most common methods of preparing perovskite nanocrystals are discussed in this section.

4.1.1 High Temperature Synthesis:

Higher temperatures are frequently used to control the colloidal syntheses' nucleation thermodynamics. The critical radius is typically enhanced by an elevated nucleation temperature, ensuring that tiny nanocrystals are stabilised with respect to redissolution. According to the same principle, temperature also serves as an easily modifiable parameter for the adjustment of nanocrystal size. Additionally, it is occasionally required to use higher temperatures to solubilize desirable precursor salts or ligands in the reaction media. Hot injection is the most popular high-temperature synthesis technique for perovskite nanocrystals.

A variety of semiconducting nanocrystals are frequently synthesised using the hot-injection approach[23]. It involves the high-temperature and inert-gas injection of one precursor solution into the other. As a result of the supersaturation of the monomers, nanocrystals form quickly and are stabilised at the nanoscale by long-chain ligands that are also dissolved in the reaction mixture. Ice water is generally used to rapidly cool the reaction vessel in order to stop additional nucleation and restrict growth. The hot-injection technique was highly intriguing for perovskites because they are known to be more susceptible to environmental deterioration and disintegration

than other semiconductor materials.

4.1.2 Room Temperature Synthesis:

Room temperature processes, particularly those carried out without stringent environmental controls, offer a more economically and commercially viable approach compared to high-temperature techniques commonly employed in the synthesis of perovskite nanocrystals. Among these methods, Ligand Assisted Reprecipitation (LARP) stands out as the most prevalent room temperature synthesis technique, characterized by its simplicity and minimal requirement of standard wet chemistry equipment. Consequently, LARP is highly amenable to scalability and holds substantial appeal for industrial applications, considering financial, energy, and procedural considerations.

In a typical LARP procedure, the perovskite precursor salts (such as PbX_2 and AX) are dissolved in a polar solvent (commonly N, N-Dimethylformamide (DMF) or Dimethyl sulfoxide (DMSO)). This solution is subsequently injected into a non-polar solvent (known as the Bad solvent or Antisolvent), creating a supersaturated state and facilitating immediate nucleation of nanocrystal formation. Prior to nucleation, organic ligands are introduced into either solvent. These ligands not only serve to prevent crystal aggregation but also promote the stable colloidal dispersion of nanocrystals in non-polar organic solvents, thanks to the extended organic chains interlocking with neighboring crystals.

4.2 Preparation of Perovskite Precursor Solution:

While Ligand Assisted Reprecipitation (LARP) offers a lower-temperature route for nanocrystal synthesis, it introduces challenges due to the incorporation of strongly coordinating solvents, such as DMF and DMSO, during the synthesis process. It is hypothesized that the presence of

residual coordinated solvents (DMF and DMSO) on the crystal surface is a contributing factor to the accelerated degradation observed in Perovskite Nanocrystals[11]. A solvent like Acetonitrile, less strongly coordinating in nature, can be useful for synthesising nanocrystals. But the Lead Halide salts are sparingly soluble in Acetonitrile. Hence we adopted a compound solvent system of methylamine dissolved in Acetonitrile (ACN/MA) reported by Noel and others in 2017[20]

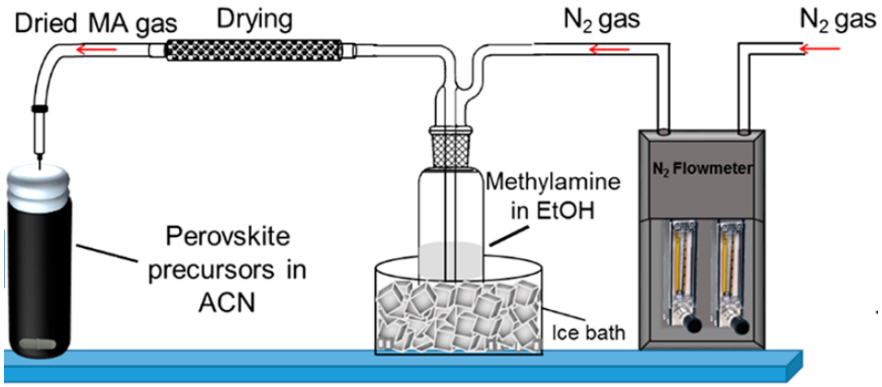

Figure 4.1: Schematic representation of the setup used for dissolving the perovskite precursor salts in Acetonitrile saturated by Methylamine gas[11].**©Adapted from references with permission**

Figure 1 illustrates an efficient method of preparing a precursor solution for perovskite nanocrystal synthesis. An aerator containing Methylamine solution (33% wt in ethanol) was degassed by passing Nitrogen gas through it and passed through a drying tube before bubbling it directly into the precursor solution of MABr and PbI_2 in ACN. The solution turned from a dark green-black dispersion into a clear, pale yellow solution after the bubbling process. The precursor solution was then saturated with MA gas and stored in a refrigerator for later use. This technique enables the preparation of a stable perovskite precursor solution for the synthesis of high-performance perovskite nanocrystals.

Chapter 5

Red Emitting Perovskite Nanocrystals:

All the synthesis processes were conducted in a fume hood under ambient conditions.

Chemicals:

Lead Iodide(PbI_2, 99% trace metal basis) was purchased from Tokyo Chemical Industries (TCI), Methylammonium Bromide(MABr) was purchased from Gratecell solar, Acetonitrile(anhydrous, 99.8%), Oleic Acid(Technical grade, 90%), Oleylamine(Technical grade, 70%), and Methyl Acetate(anhydrous, 99.5%) were purchased from Sigma-Aldrich and used without further purification.

5.1 Preparation of $MAPb(I_{1-x}Br_x)_3$ Perovskite Precursor Solution:

Methylammonium bromide(MABr) and Lead Iodide (PbI_2) were used to get the $MAPb(I_{1-x}Br_x)_3$ Perovskite Precursor Solution. Typically, in a 15ml vial, 2 millimoles of PbI_2 (922mg) and 2 millimoles of MABr (224mg) were mixed with 4ml of anhydrous Acetonitrile(ACN). The resulting suspension was kept for stirring until a dark-green-black dispersion was formed. Then, the dried methylamine gas was passed into the dispersion following the setup described in the previous section. After bubbling the methylamine gas into the black dispersion for a certain time, the solution turned into a clear, translucent pale yellow solution, thus dissolving the salts completely. To avoid

further precipitation of the salts, it was made sure that the solution was saturated with methylamine gas. Then, the solution was sealed and kept in a refrigerator until further use.

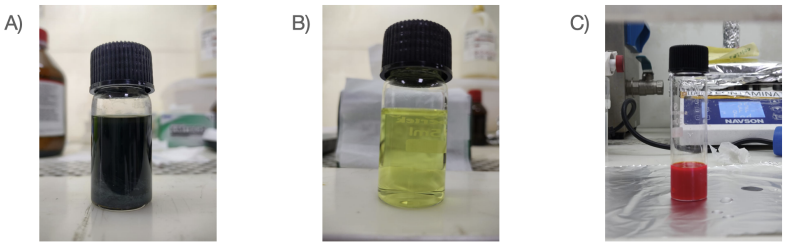

Figure 5.1: A) Black dispersion of Precursor Salts in ACN. B) Translucent Pale Yellow after bubbling MA gas. C) As synthesized Nanocrystals.

5.2 Synthesis of $MAPb(I_{1-x}Br_x)_3$ Perovskite Nanocrystals:

The usual Ligand Assisted precipitation method was followed for preparing nanocrystals, as shown in Fig 5.2

A vial containing a mixture of 5ml of Toluene, 1.8ml of Oleic Acid, and 0.2ml Oleylamine was kept stirring vigorously at 60 ^{o}C. Then, 0.2ml of perovskite precursor solution was injected into this hot mixture while maintaining vigorous stirring. The suspension immediately turned red, indicating the nanocrystals' nucleation. The reaction was continued for 90s, allowing a uniform crystal growth before quenching the reaction by immersing this vial into an ice bath.

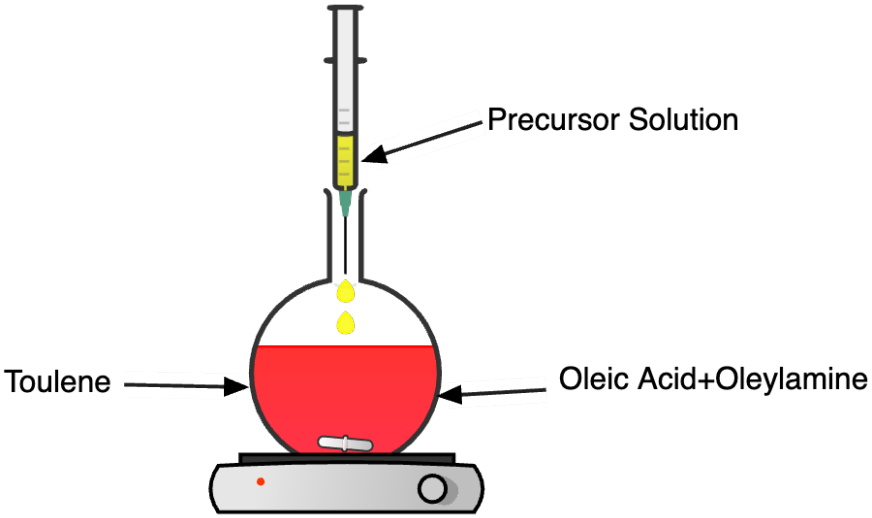

Figure 5.2: Schematic representation of Ligand Assisted Reprecipitation method

5.3 Nanocrystal Isolation:

The Nanocrystals were precipitated by adding 15ml of Anhydrous Methyl acetate. The excess amount of unreacted ligands and precursors were removed by purifying the nanocrystals by centrifugation at 8000rpm for 10 minutes. This process was repeated twice by adding an appropriate amount of toluene to redisperse the nanocrystals and methyl acetate to precipitate them. After three purification cycles, the final precipitate was redispersed in 1 ml of Toluene.

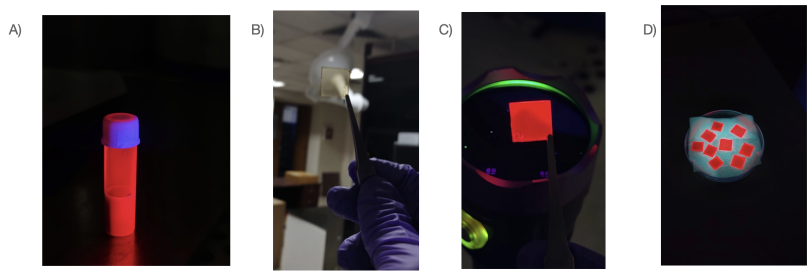

Figure 5.3: A) $MAPb(I_{1-x}Br_x)_3$ Nanocrystals colloidal solution under UV Light. B) Perovskite thin film coated on glass substrate. C) & D) Perovskite films under UV Light

5.4 Optimization of the ligands:

In the LARP method, the size of the nanocrystals is governed by the amount of surface capping ligands added into the antisolvent mixture during the reaction. Typically long chain alkylamines(Oleylamine in our case) are added to prevent direct crystallization of $MAPb(I_{1-x}Br_x)_3$ into large micrometer size crystals when the precursor solution is injected into the antisolvent(Toluene in our case) and Oleic acid is added to suppress the aggregation of synthesized Perovskite nanocrystals. Oleic Acid also helps in controlling the crystallization rate and size of the nano-particles by covering their surface.

So we studied the effect of Oleic acid concentration on the emission of the nanocrystals. Then we did the Photoluminescence study of the thin films of these nanocrystals. The films were prepared via spin coating the solution onto a cleaned glass substrate using a Navson spin coater inside a fume hood.

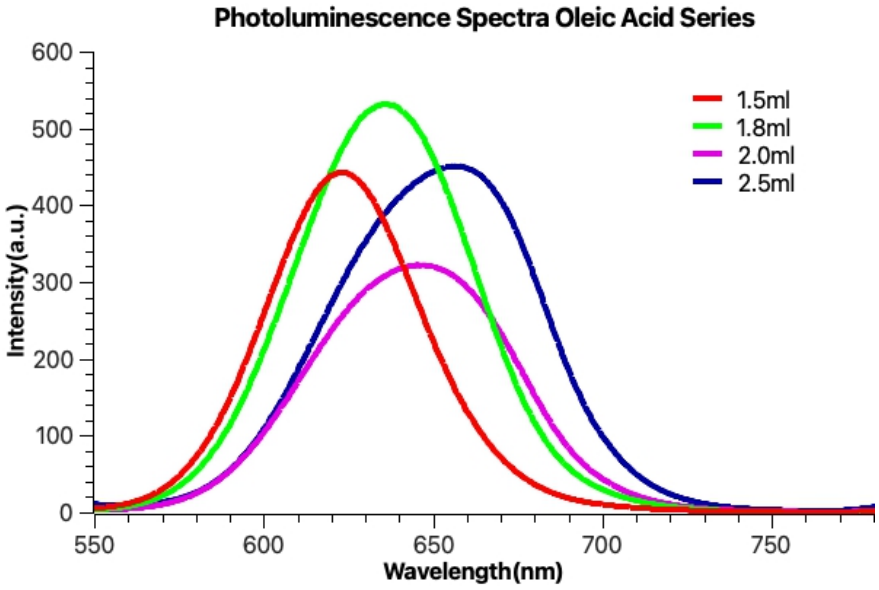

Figure 5.4: Photoluminescence spectrum: Oleic Acid Series

5.5 Nanocrystals Purification:

For Nanocrystals to be free of reaction excesses and byproducts, effective antisolvent purification is necessary. A commercial Nanocrystals ink needs to have very little impurities and be extremely reproducible. It is essential to remove excess ligands for applications involving electronic devices. This is due to the fact that these ligands are often poorly conducting organic compounds. Consequently, the extra ligand will hinder current flow and lower device performance—though maybe not consistently. Moreover, ligands are frequently oily and viscous, which means that an excess of them can change the thin-film's and solution's physical characteristics.

In our attempts to purify the nanocrystals we studied the effect of washing the nanocrystals with a well reported antisolvent Methyl acetate. We performed UV-Vis absorption spectroscopy and Photoluminescence measurements. The following graphs show PL and UV-Vis absorption of perovskite films prepared by spin coating the Perovskite Nanocrystals at each washing step.

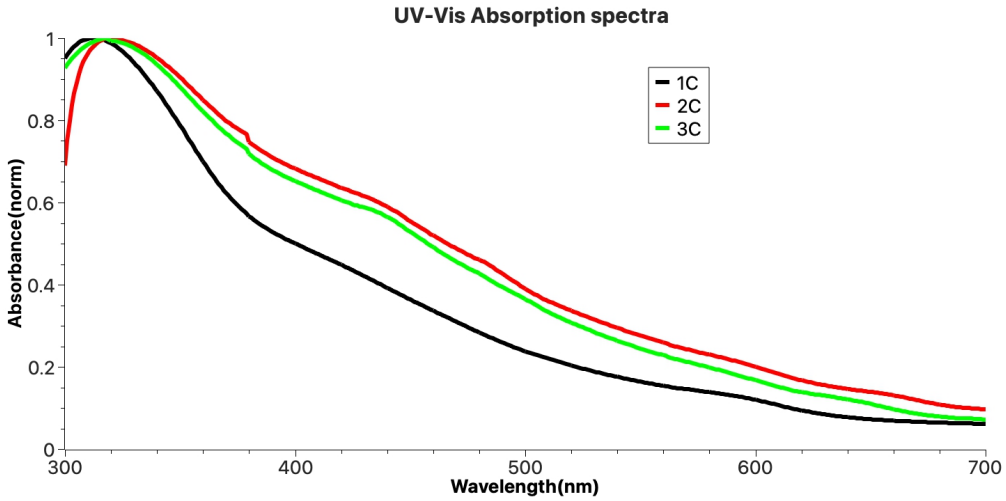

Figure 5.5: Effect of antisolvent washing cycles on UV-Vis Absorption spectra of Red NCs

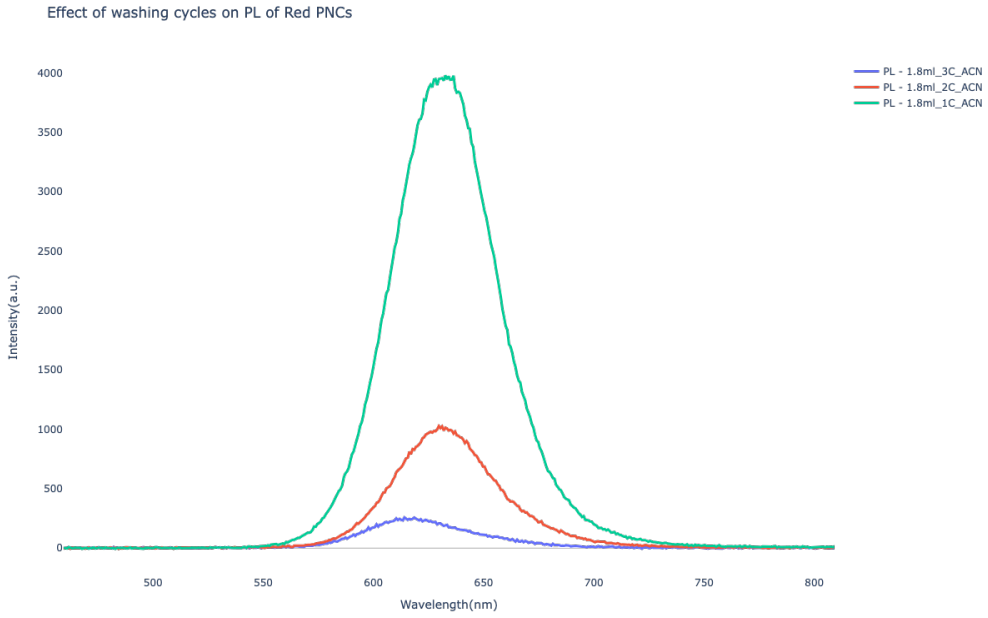

Figure 5.6: Effect of antisolvent washing cycles of Perovskite NCs on the Emission profile

5.6 Results:

We dissolved the perovskite precursor salts Lead Iodide and Methylammonium bromide using the MA/ACN compound solvent system. We then proceeded to the synthesis of red-emitting perovskite nanocrystals using a Ligand Assisted re-precipitation method and performed the optimization of ligands using Photoluminescence spectroscopy(see Fig 5.4). Simultaneously PLQY measurements were performed using the setups discussed in previous chapters.

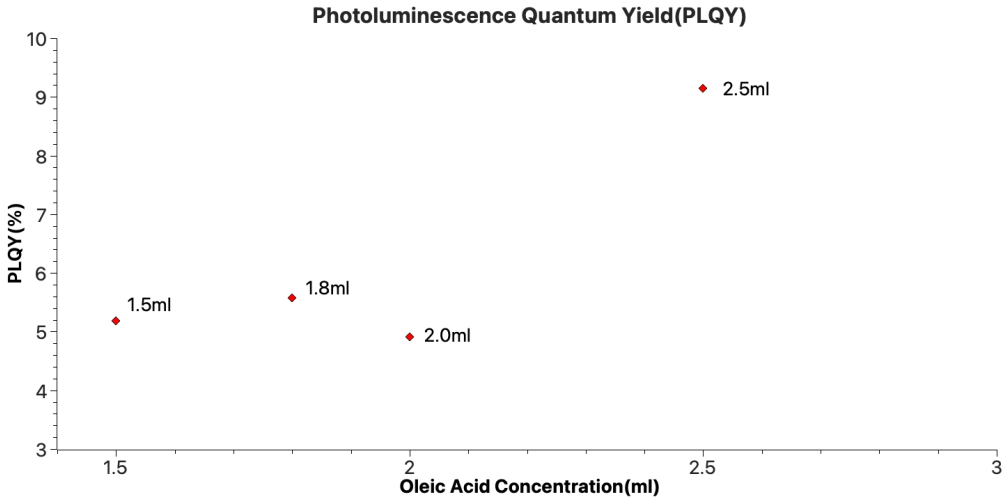

Figure 5.7: Effect of Oleic Acid Concentration on PLQY of Red NCs

In order to confirm the structure of the material prepared, we performed X-ray diffraction studies. The XRD pattern of these nanocrystals is shown in Fig. 5.8

We also studied the effect of antisolvent washing cycles to remove the excess unreacted materials and ligands which hinder the device performance of these nanocrystals. The optical absorption and emission profiles are shown in Fig 5.5 and Fig 5.6

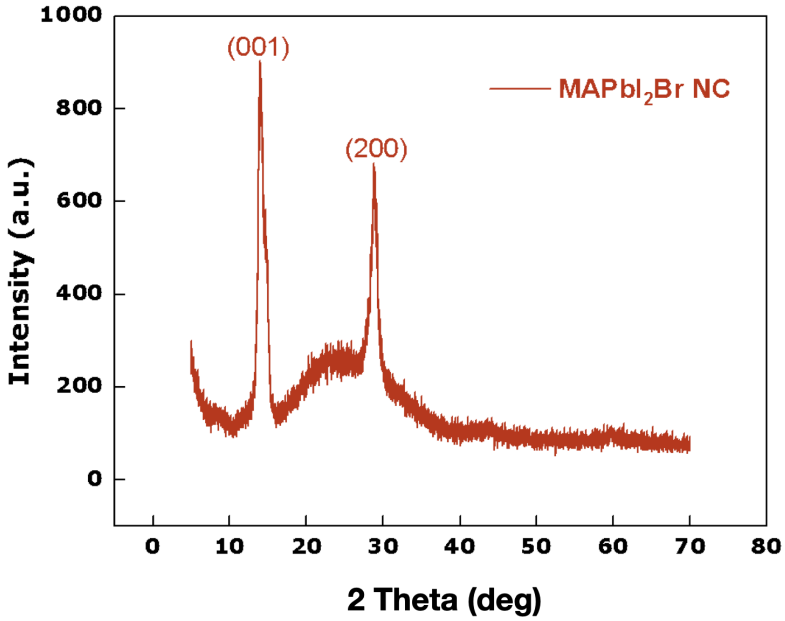

Figure 5.8: X-Ray Diffraction pattern of $MAPbI_2Br$ Nanocrystals

5.7 Conclusion:

We successfully employed the Methylamine/Acetonitrile compound solvent system for the preparation $MAPb(I_{1-x}Br_x)_3$ Perovskite precursor and were able to synthesis the nanocrystals using LARP method. We studied the evolution of PL and PLQY with change in Oleic Acid concentration. At 1.8ml Oleic Acid we got the highest intensity, a decent PLQY and emission peak at 635nm which is pure Red according to television standards. Hence we fixed the concentration of Oleic Acid at 1.8ml. We studied the effect of antisolvent washing and nanocrystals purification in order to get a working Light Emitting Diode. We found that, there is a significant loss in the Photoluminesccence(PL) intensity with the increase in washing cycles, but we got a working LED with 3 cycle washed nanocrystals(which will be discussed in chapter 7), which indicated that it is very crucial to get rid of excess ligands which are electrically insulating in nature.

Chapter 6

Towards Green-Blue Nanocrystals:

To get stable green and blue emitting nanocrystals via Ligand Assisted Reprecipitation we prepared a few precursor salts which can be used for successful demonstration of non-coordinating solvent approach. These experiments and subsequent results will be addressed in this chapter. All of the processes mentioned here were carried out inside a fume hood.

Chemicals:

Lead Bromide($PbB_{2,}$ 99% trace metal basis) was purchased from Tokyo Chemical Industries (TCI), Methylammonium Bromide(MABr) and Methylammonium Chloride(MACl) was purchased from Gratecell solar, Hydrobromic acid(HBr, 48%), Hydrochloric Acid(HCl, 37%), Toluene (anhydrous),Acetonitrile(anhydrous, 99.8%), Oleic Acid(Technical grade, 90%), Oleylamine(Technical grade, 70%), and Methyl Acetate(anhydrous, 99.5%) were purchased from Sigma-Aldrich and used without further purification.

6.1 Challenges in getting a Precursor solution

In previous chapters we have shown that the compound solvent system of Methylamine/Acetonitrile can be used to dissolve the perovskite precursors. But applying this non-coordinating solvent approach to the Bromide and Chloride precursor is not that easy. The dissolution procedure utilized for CH3NH3PbBr3 is not directly transferable, given its tendency to yield an unstable precursor

solution[21]. In this context, we have implemented an adapted method to disperse $MAPbBr_3$ precursor salts within acetonitrile (ACN). By saturating the solution with methylamine (MA) gas, the precursor salts effectively dissolve, resulting in the creation of a stable, transparent, and colorless solution.

6.2 Preparation of hybrid halide compound $DMAPbBr_3$

In 2015 Wang and others reported a new precursor salt named '$HPbI_3$'[28] for Lead Halide Perovskites which was formed by the reaction between Lead Iodide(PbI_2) and Hydroiodic acid(HI). Earlier which was supposed to be a hydrogen atom indeed turned out to be dimethylammonium ion(DMA). This Dimethylammonium cation comes into the picture due the acidic hydrolysis of *N,N'* Dimethylformamide.

In 2018 Nakita Noel and others modified this approach to the bromide system and they showed that it is possible to get a stable $MAPbBr_3$ perovskite precursor in Methylamine/Acetonitrile solvent system[21] if we use $DMAPbB_3$ instead of lead bromide and Methylammonium Bromide as the perovskite precursors. They also demonstrated the fabrication of efficient solar cells based on this perovskite solution. To prepare stable Green emitting Perovskite naocrystals via Ligand ligand-assisted re-precipitation method and follow the non-coordinating solvent it becomes very crucial to get a stable perovskite precursor solution. So we followed the methodology mentioned above as a way to dissolve perovskite precursor salts.

Typically in this process, $PbBr_2$ and HBr were mixed into DMF at a molar ratio of 1:1.5 . The reaction was kept for continuous stirring at 50 °C for 3 hours. After 3 hours, a supersaturated solution was formed. This solution was left to cool down naturally and kept inside a refrigerator overnight. The next day, the powder was filtered out from the solution via vacuum filtration using Diethyl ether and the remaining supernatant was discarded. It is made sure that the powder is dried out completely and no moisture resides inside. The powder is then dried under vacuum and stored

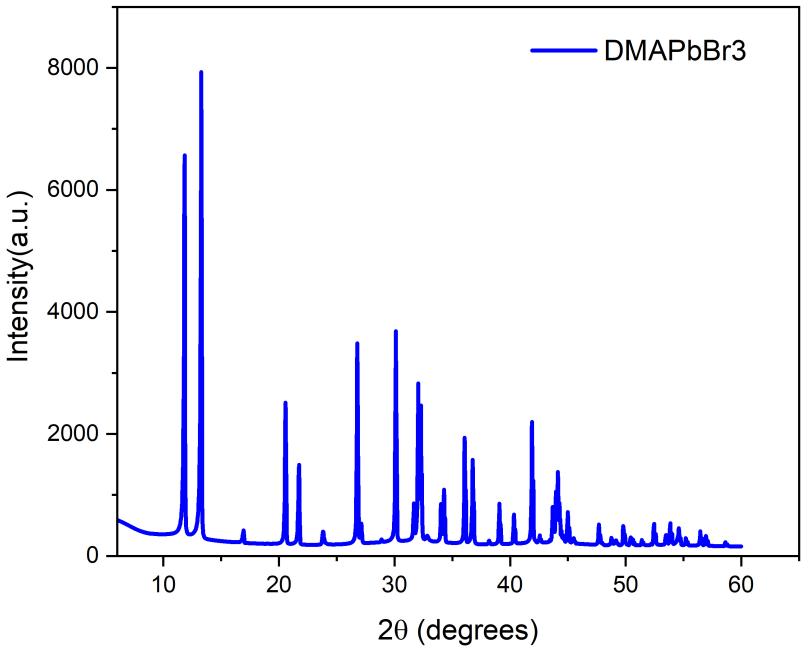

Figure 6.1: X-Ray Diffraction pattern of $DMAPbBr_3$

inside a glovebox under nitrogen atmosphere.

6.3 Preparation of $MAPbBr_3$ Perovskite Precursor solution:

In a glass vial equimolar amounts (1millimole each)of Methylammonium bromide(MABr) and $DMAPbBr_3$ were mixed with 1ml of Anhydrous acetonitrile. The mixture was kept for stirring and it formed an orangeish dispersion. Then the dried methylamine gas was brought to saturate this dispersion through the setup as described in the previous chapters. As we started to bubble the dried methylamine gas into this orange dispersion it soon started to dissolve the salts and a clear and transparent solution was formed indicating the complete dissolution of perovskite salts. This

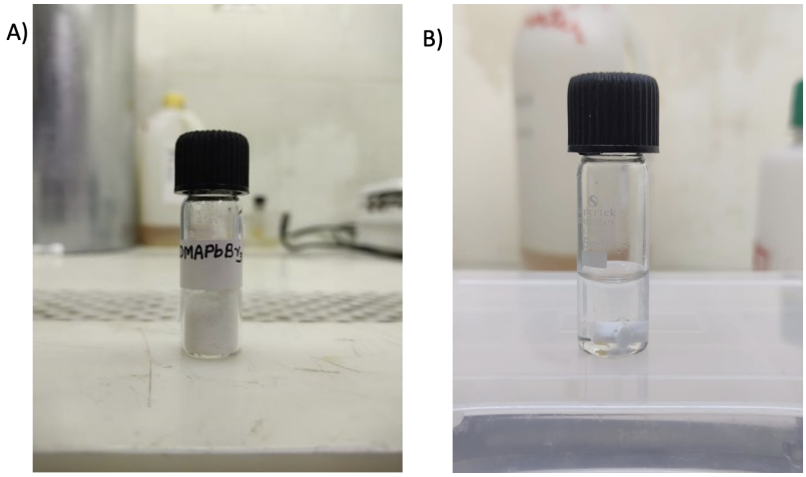

Figure 6.2: A) As prepared powder of $DMAPbBr_3$. B) Completely dissolved precursor solution of $MAPbBr_3$ via MA/ACN compound solvent system.

solution was then sealed and kept inside the refrigerator until future use.

6.4 Preparation of $MAPbBr_3$ Nanocrystals and Ligand Optimization

The $MAPbBr_3$ nanocrystals were prepared via a typical Ligand Assisted Reprecipitation method as shown in the following fig 6.3.

We prepared Nanocrystals via LARP and as we knew from our previous experience with Red NCs, we simultaneously tried to optimize the amount of Oleic acid. We prepared NCs with 3 different concentrations of Oleic Acid. So, in 3 vials containing 5ml of anhydrous toluene, we added 1.2ml, 1.8ml and 2.4ml of Oleic acid respectively and 0.2ml of Oleylamine in each of the three vial. This reaction mixture was kept for a vigorous stirring at 60 degrees. Then 0.2ml of $MAPbBr_3$

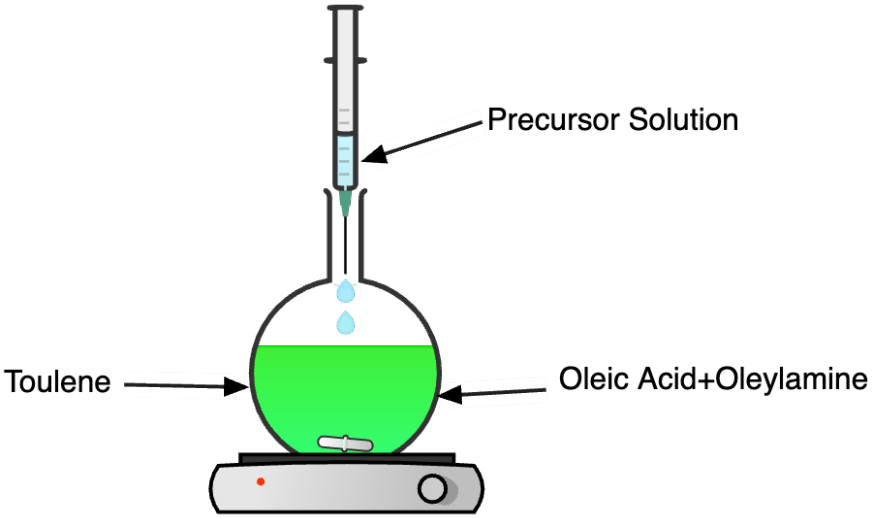

Figure 6.3: Preparation of $MAPbBr_3$ nanocrystals via LARP method

precursor prepared as mentioned before, was swiftly injected into the reaction mixture. The reaction mixture was kept stirring continuously till 90s before quenching the reaction by keeping the vials in the ice bath.

6.5 Optimization of $MAPbBr_3$ Perovskite nanocrystals via reaction temperature and time:

Reaction temperature and time before stopping the reaction plays significant role in governing the size and shapes of the nanoparticles. Hence we Prepared Nanocrystals at different temperatures keeping the time constant and studied their Photoluminescence properties in order to get a blue shift through quantum confinement. The same process was repeated keeping the reaction temperature fixed and by varying the time before quenching the reaction.

The following figures show the Photoluminescence spectra of the time series and temperature

series for $MAPbBr_3$ nanocrystals.

6.6 Preparation of hybrid halide compound $DMAPbCl_3$

After the successful synthesis of Green emitting nanocrystals from an organic inorganic hybrid halide compound $DMAPbBr_3$ we prepared a new hybrid compound $DMAPbCl_3$ following a similar process mentioned in the previous sections of this chapter. In this process, Lead Chloride($PbCl_2$) and Hydrochloric acid were dissolved in *N,N'* Dimethylformamide at a molar ratio of 1:1.5. The reaction is then kept for continuous stirring at 50 degree celsius for 3 hours. After 3 hours a white supersaturated solution was formed. This solution was then left to cool down naturally and was then stored in the refrigerator overnight. The $DMAPbCl_3$ powder was then filtered out of the solution via vacuum filtration using diethyl ether. The white powder is then dried under a vacuum to remove any remaining moisture residues. The $DMAPbCl_3$ powder was then stored under a nitrogen environment inside a glovebox.

6.7 Preparation of $MAPbCl_3$:

In a glass vial, equimolar quantities(1millimole each) of $DMAPbCl_3$ and Methylammonium chloride(MACl) were mixed with 1ml of anhydrous acetonitrile. The solution was kept for continuous stirring and then the dried methylamine gas was bubbled with the setup described previously to form the Methylamine/Acetonitrile compound solvent system. But the solution soon started to look turbid and initiated the settling down of a white precipitate. Which indicated that the salts are insoluble in this particular solvent system.

6.8 Results:

The results of the experiments carried out for the preparation and synthesis of green-emitting perovskite nanocrystals will be briefly discussed here.

The following figure shows evolution of Photoluminescence spectra with the variation in the ligand (Oleic Acid) concentration. We prepared the nanocrystals using different amounts of oleic acid in the reaction mixture. The change in PL can be understood by fig. 6.4

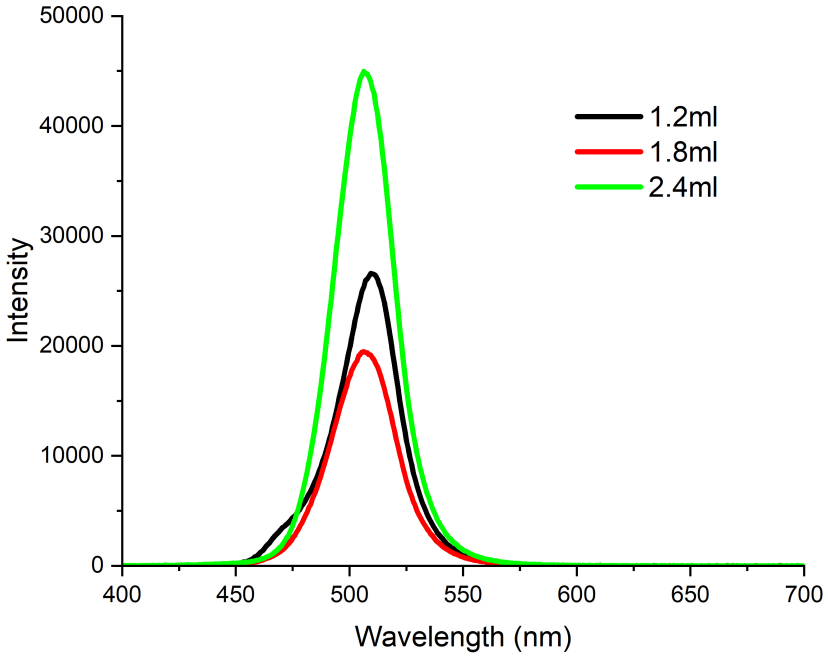

Figure 6.4: Photoluminescence Spectrum: Oleic Acid series for $MAPbBr_3$

Simultaneously we performed measurements of the Photoluminescence Quantum Yield(PLQY) following the techniques described in Chapter 3. The effect of concentration of Oleic acid is evident in the values of PLQY we got and can be understood by studying the following plot.

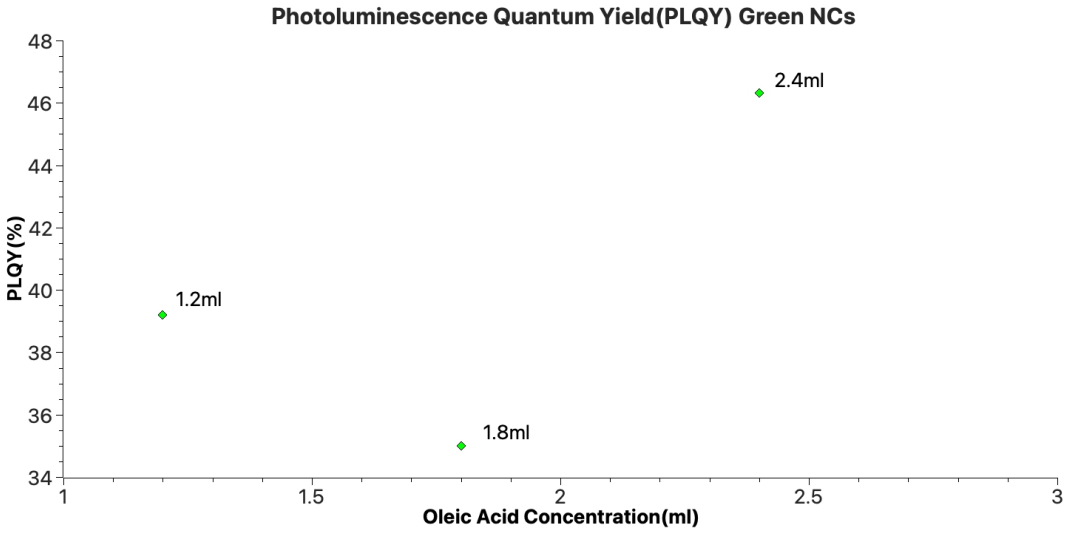

Figure 6.5: Effect of Oleic Acid concentration on PLQY of Green Perovskite NCs

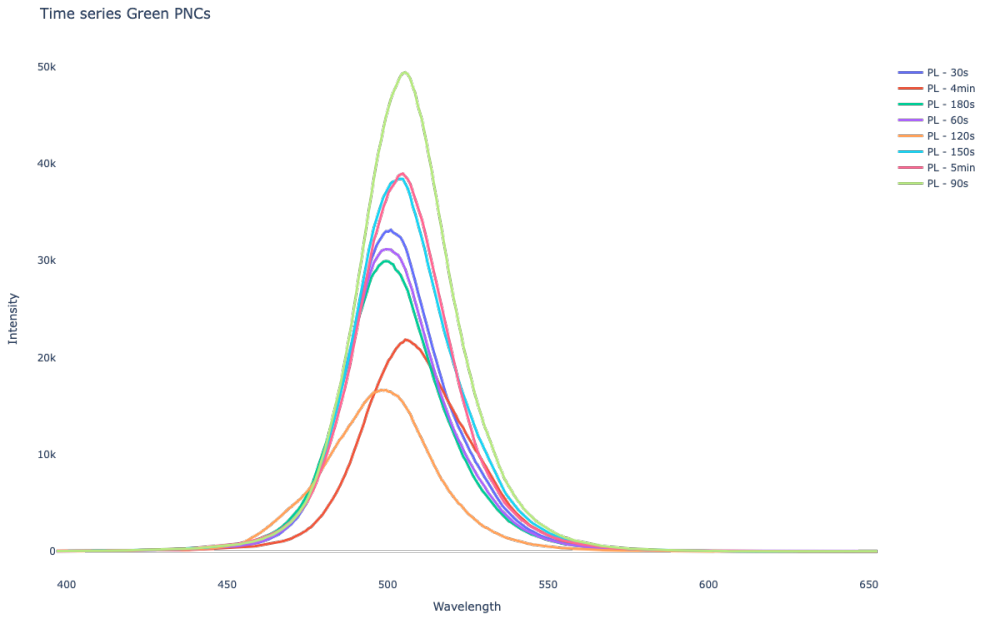

Figure 6.6: Photoluminescence Spectrum: Time series

To get a better understanding of the kinetics and growth of Nanocrystals, and to achieve Blue emission by means of quantum confinement, we studied the effect of nanoparticle growth and size governing parameters such as Time(Fig.6.6) and Temperature(Fig.6.7).

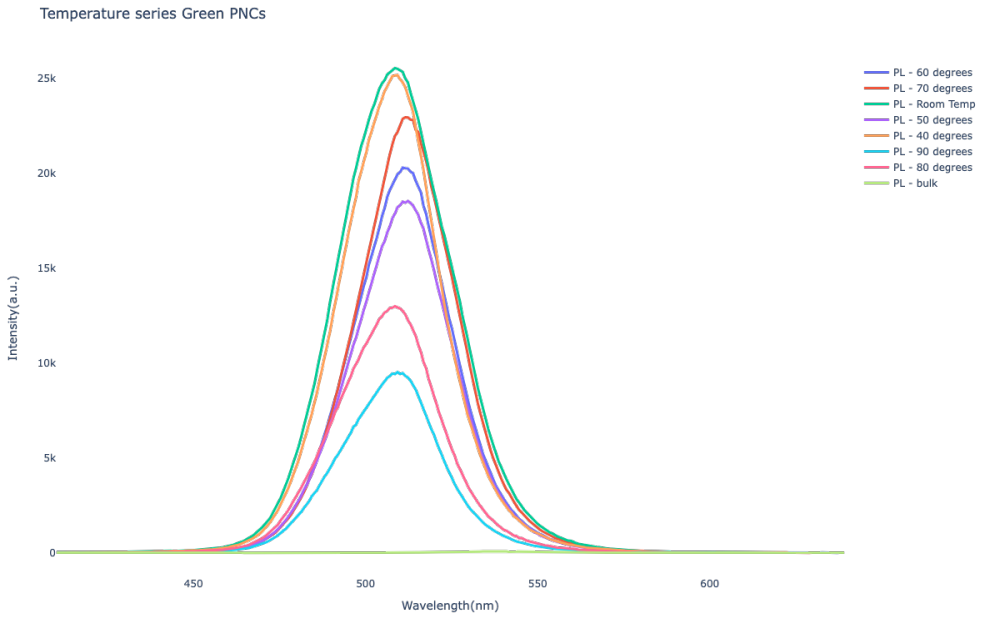

Figure 6.7: Photoluminescence Spectrum: Temperature series

6.9 Conclusions:

We prepared a hybrid lead halide compound $DMAPbBr_3$ and employed it as a Lead(Pb) source in the precursor. In this way we can employ our non-coordinating solvent approach to dissolve the precursor salts in MA/ACN compound solvent system. We successfully achieved a stable and completely dissolved $MAPbBr_3$ precursor solution in Acetonitrile. The Green emitting Per-

ovskite Nanocrystals were prepared via Ligand Assisted re-precipitation method. Simultaneously the amount of ligands (Oleic Acid) was fixed to 2.4ml by studying the emission spectrum and PLQY of the thin films made with these nanocrystals. We got the maximum PL intensity with 2.4ml of Oleic Acid and emission peak at 510nm; also the films with 2.4ml of ligand concentration had the highest PLQY of 46.31% concluding that the surface is well passivated.

In order to get blue emission through quantum confinement we studied the nanocrystals' size governing parameters such a time and temperature but we didn't get any conclusive data.

Also we tried to get $MAPbCl_3$ solution via MA/ACN compound solvent system but couldn't succeed. So, we were unable to employ the Methylamine/Acetonitrile compound solvent system to achieve Blue emitting nanocrystals. Further studies needed to be done in this regard.

Chapter 7

Device Fabrication:

7.1 A Brief History:

Although the initial LED devices based on perovskite materials were developed in the year 1994[6], it wasn't until 2014[27] that the first working PeLED at room temperature was developed. The highest EQE of Perovskite Light Emitting Diodes (PeLED) has climbed from 0.76% to nearly 25% since then and is predicted to rise even further. PeLEDs offer a lot of interesting features. As previously discussed in the preceding sections, the color output of PeLEDs can be precisely tuned across the entire visible light spectrum, spanning approximately 400 to 800 nm. Furthermore, in comparison to alternative LED technologies, PeLEDs exhibit an exceptionally narrow emission profile, characterized by a reduced Full Width at Half Maximum (FWHM), thereby facilitating the production of highly pure-color LEDs.

Perovskite LEDs offer an additional advantage over alternative emissive materials through their ease of fabrication. The precursor materials for perovskites are abundant on Earth, ensuring a readily available and cost-effective supply, which further enhances the appeal of PeLEDs. Perovskites are amenable to solution processing, characterized by a relatively low defect density and a high tolerance for imperfections. In contrast to certain OLED emitters necessitating thermal evaporation in high vacuum conditions, solution processing is not only more efficient but also cost-effective. Moreover, the lower production temperatures required for perovskite LEDs contribute to energy savings and enable the use of flexible substrates like polyethylene terephthalate (PET), with a lower

melting point of approximately 250°C.

7.2 Device architecture and various layers

The fundamental architecture of an LED comprises a layer of light-emitting material interposed between two electrodes. For efficient light emission from the device, one of these electrodes must be transparent. Typically, additional functional layers are incorporated between the electrodes and the light-emitting layer to enhance LED performance. The electron transport layer (ETL) serves the purpose of facilitating the movement of electrons from the cathode to the perovskite conduction band, while the hole transport layer (HTL) facilitates the transport of holes from the anode to the perovskite valence band.

Within the perovskite layer, the recombination of holes and electrons culminates in light emission. In certain cases, to prevent the unwanted leakage of holes and electrons in the opposite direction, either an electron-blocking layer (EBL) or a hole-blocking layer (HBL) may be incorporated. Beyond these functional layers, the LED assembly also encompasses a substrate material on which the device is constructed.

There are two possible configurations for the devices: either the other way, or the substrate side can be used to inject holes and electrons. The names of the structures are n-i-p and p-i-n, where i stands for intrinsic, n for negative, and p for positive.

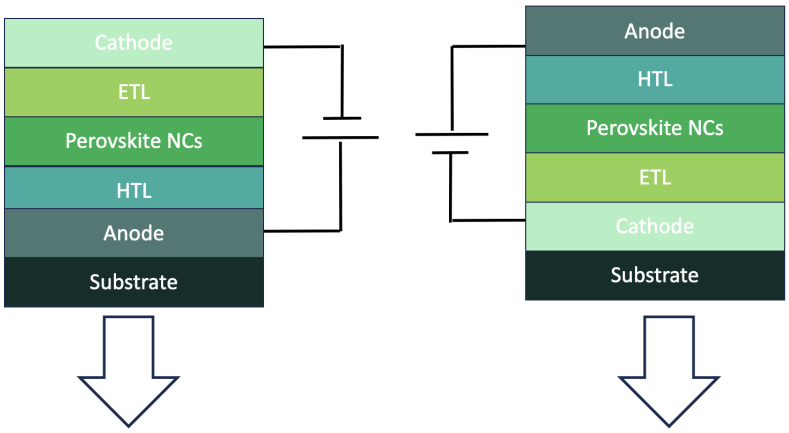

Figure 7.1: p-i-n (left) and n-i-p (right) device architectures used in PeLEDs

7.2.1 Transparent Conducting Oxide

Glass serves as the predominant substrate material upon which these LED devices are constructed. The escape of emitted light from the device typically occurs through the substrate, necessitating transparency, at the very least, within the wavelength range of the emitted light. Since the emitted light traverses through the lower electrode, a requisite level of transparency is essential. Presently, the cutting-edge conducting electrodes employed are Indium-doped Tin Oxide (ITO) and Fluorine-doped Tin Oxide (FTO).

7.2.2 n-type metal oxides

Transition metal oxides are an intriguing class of inorganic solids with a diverse range of structures and characteristics. They have been used extensively as transparent electrodes and non-ohmic resistors because of their unique combination of optical and electrical qualities, which include high electrical conductivity and great transparency in the visible spectrum. These properties also make them useful in electro-optical systems. Zinc Oxide (ZnO), which has a large bandgap of

around 3.3 eV and can transport electrons through oxygen vacancies driven on by lattice defects, was employed in our devices as an electron transport layer. ZnO was prepared by dissolving 109 mg of Zinc acetate dihydrate in 1 ml of 2-methoxy ethanol and 30 microlitres of ethanolamine.

7.2.3 p-type organic materials

4,4'-Bis(N-carbazolyl)-1,1'-biphenyl (CBP) is one of the widely used hole-injecting material for efficient Green and Red Perovskite Light-Emitting Diodes. It is due to its deep-lying HOMO (-6.0 eV) enables the confinement of charges inside the perovskite layer and prevents leaking of charges. We prepared a 10mg/ml concentrated solution prepared in Chlorobenzene for our devices.

A triarylamine-based semiconductor, called Poly(9,9-dioctylfluorene-alt-N-(4-sec-butylphenyl)-diphenylamine) (TFB), has a band gap of 3.0 eV (HOMO and LUMO levels of 5.3 and 2.3 eV, respectively), and a comparatively high hole mobility of 2 $\times 10^{-3}$ cm^2 V^{-1} s^{-1}. We prepared a 10mg/ml concentrated solution prepared in equal amounts of Chlorobenzene and Chloroform for our devices.

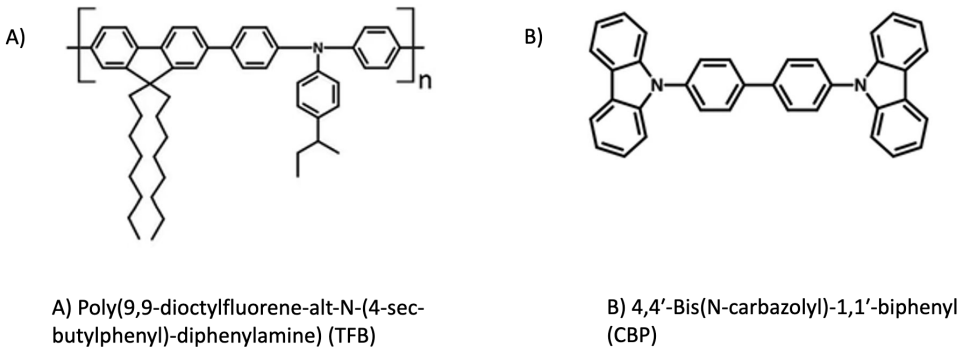

Figure 7.2: Structures of TFB and CBP

7.2.4 Top Electrode

The principal prerequisites for a material to qualify as a top electrode are its electrical conductivity and an appropriate work function. Enhancing the illuminance of an LED can be achieved through the implementation of a reflective top electrode, which effectively reflects the emitted light. Conversely, transparent LEDs are made possible by the translucent top electrode. As the top electrode is deposited last under high temperature and high vacuum, the other layers must be able to tolerate these conditions. Commonly used top electrode materials are Gold(Au), Silver(Ag) and Aluminium(Al). We used a high work function metals such as Gold(Au) as an anode(Top Electrode) along with a thin layer of p-type metal oxide such as MoO_3 which is thermally deposited between gold and hole injecting layers.

7.3 Fabrication of Red Perovskite LEDs:

Red Perovskite LEDs were fabricated via solution processing methods using $MAPb(I_{1-x}Br_x)_3$ nanocrystals prepared by LARP method mentioned in chapter 5.
Indium Tin Oxide(ITO) coated glass substrates were cleaned with Soap water followed by DI water, Acetone and Isopropyl alcohol by ultrasonication. Then substrates were further cleaned via UV-Ozone plasma treatment.

7.3.1 Depositing Electron Injecting Layer ZnO:

The cleaned substrates were then transferred into fume hood and a freshly prepared solution of Zinc Oxide (ZnO) was spin-coated on these glass substrates using a NAVSON spin coater. The substrates were then annealed for 10 minutes at 200 degrees on a NAVSON hotplate.

Figure 7.3: A n-i-p device architecture for our Red Perovskite LEDs

7.3.2 Emissive layer:

For ease in the fabrication of devices, we blended our Perovskite nanocrystals with the hole-injecting layers TFB and CBP to build a host-guest matrix. It was always a problem to get good and balanced hole injection in the perovskite emissive layer due to the low-lying Valence band and as the subsequent layers on the perovskite nanocrystals need to be thermally evaporated under high vacuum, which hinders the device performance as there's always a debate on the thermal stability of perovskites. Hence, using a blend of emissive layers with hole-injecting layers offers an easy, low-cost and time-consuming, scalable and efficient way of fabricating the devices.

We prepared a blend of Perovskite Nanocrystals, CBP, TFB in a ratio of 2.5:1:1. The solutions were prepared inside a N_2 filled Mbraun Glove box. Then, the ZnO-coated ITO substrates were transferred into the glove box. The blended emissive layer was then spin-coated using the integrated spin-coater inside the glove box. Typically 40 microlitres of perovskite solution was spread evenly on the substrate and was spin-coated at 1500rpm for 30s followed by a drying step of spinning the

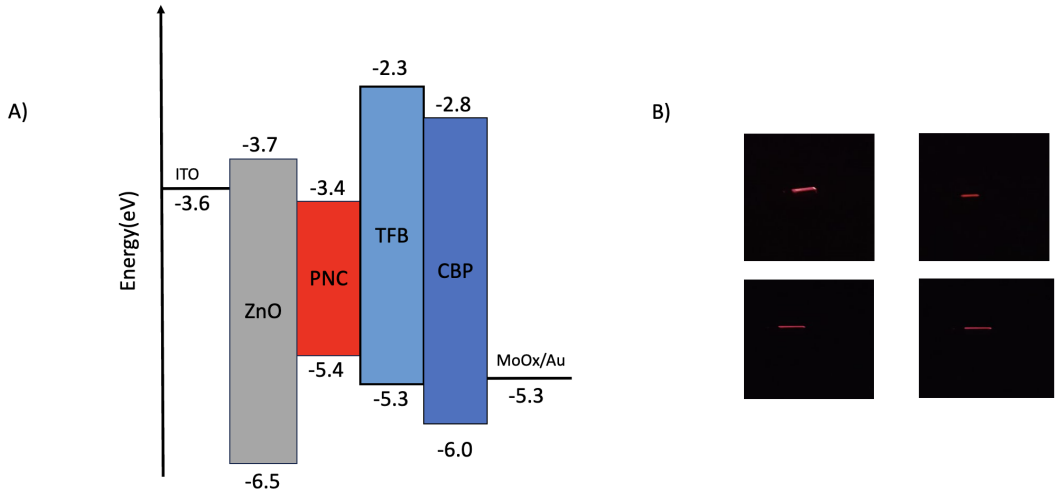

Figure 7.4: A) Energy band diagram of different layers in Red Perovskite LED. B)Snippets of Glowing Red LEDs under electrical bias

substrate at 3000rpm for 60s.

7.3.3 Deposition of top electrode:

The perovskite nanocrystals coated substrates were then transferred into a Thermal Evaporator(Angstrom Engineering) for depositing a very thin layer(10nm) of p-type metal oxide MoO_x under high vacuum conditions with a very slow deposition rate. MoO_x has a high refractive index (n_x=1.9) and a LUMO level at -6.9eV which ensures an ohmic contact with the perovskite materials.
The substrates were then transferred into another thermal evaporator (VR Technologies) for deposition of gold(Au) electrode. A 100nm thick layer of gold was deposited under high vacuum and a slow deposition rate was ensured.

7.4 Results and Conclusion:

These fabricated Perovskites LEDs were tested by applying electrical bias using a Keithley 2400 sourcemeter. These LEDs started glowing at an average turn-on voltage of 1.8V(see Fig). The LEDs glowed for more than 1 minute on average. We are still setting up the characterization tools for the measurements, so that we can evaluate the External Quantum Efficiency(EQE), Luminance and other characteristic properties.

Although we got a working Red Perovskite LED, we are yet to get a working Green Perovskite LED. We are investing our time in device engineering for the same, and this would be the future course of the work of this project.

Chapter 8

Challenges and Limitations:

8.1 Challenges:

Over the course of just a decade, the External Quantum Efficiencies (EQE) of green and red Perovskite Light Emitting Diodes (PeLEDs) have exhibited remarkable advancements, outpacing the progress seen in OLEDs and QLED technologies. Presently, the reported EQEs for Green and Red PeLEDs exceed 28% and 25%, respectively[33]. Notably, Blue PeLEDs often incorporate mixed bromide and chloride anions, which, regrettably, are susceptible to 'Halide-Segregation' issues under photoexcitation or electrical bias. The initial challenge lies in achieving a stable perovskite solution with these mixed halides, a non-trivial task. Moreover, an elevated chloride content results in a higher exciton binding energy, leading to an increased incidence of non-radiative recombinations that ultimately diminish the final Photoluminescence Quantum Yield (PLQY) and adversely impact device performance.

Although, LARP method is easy to scale up for the fabrication of Red and Green Perovskite Nanocrystals based Light Emitting Diodes. It is very difficult to get true-blue(below 450nm) emitting nanocrystals. We have to investigate further in order to get suitable and soluble precursor salts similar to these hybrid halide compounds(eg., $DMAPbBr_3$ and $DMAPbCl_3$). Also as we observed in our experiments, we need to investigate various solvent combinations to get a compound solvent capable of forming a stable perovskite precursor solution. There are some Quasi-2D Perovskite which have been being used in blue-emitting PeLEDs due to ease of confining charge carriers in-

side the emissive layer via quantum confinement but due to the presence of long chain organic spacer cations which are generally insulating in nature, the conducting properties are not up to optimum.

The advancement of Perovskite Solar Cells serves as a foundational catalyst for much of the ongoing research in PeLED technology. In solar cells, the ideal band gap for an absorbing material resides in the infrared spectrum, typically at 1.35 eV (918 nm). Consequently, Electron Transport Layers and Hole Transport Layers, initially developed for Perovskite solar cells, have found applications in Red and IR PeLEDs. However, as the bandgap increases, issues arise with band alignment. Hence, the quest for effective charge transport materials becomes imperative for Blue PeLEDs. The deep valence band characterizing blue-emitting materials poses challenges for hole injection, necessitating the exploration of novel materials capable of serving as effective transport layers.

Although the efficiency of green and red PeLEDs currently outshines that of Blue PeLEDs, they still lag behind state-of-the-art technologies like OLEDs and QLEDs. Nevertheless, it is essential to acknowledge that Perovskite LED technology is in its infancy relative to these established technologies, and the current findings are promising. Further enhancements in PeLED efficiency can be achieved through meticulous optimization of structures and interfaces, fostering balanced and efficient charge injection within the emitter layer.

8.2 Limitations:

Although the method used by us i.e., Methylamine/Acetonitrile compound solvent system followed by LARP showcases a highly scalable way to get stable and efficient Perovskite Nanocrystals, there are also certain limitations to this method. As described in the chapter 6, we couldn't get a precursor solution for the preparation of Blue emitting perovskite nanocrystals. So this method, as of now can only be used for the synthesis of Green and Red Perovskite nanocrystals.

Further, through this method we can only produce the Methylammonium based Perovskites and we cannot produce the Ceasium or Formmamidinium based perovskites and subsequent nanocrystals. So, although being a robust method this is not universally applicable method.

Bibliography

[1] Quinten A Akkerman, Gabriele Rainò, Maksym V Kovalenko, and Liberato Manna, *Genesis, challenges and opportunities for colloidal lead halide perovskite nanocrystals*, Nat. Mater. **17** (May 2018), no. 5, 394–405 (en).

[2] A P Alivisatos, *Perspectives on the physical chemistry of semiconductor nanocrystals*, J. Phys. Chem. **100** (January 1996), no. 31, 13226–13239 (en).

[3] P K Bhatnagar, *Organic light-emitting diodes—a review*, Advanced structured materials, 2018, pp. 261–287.

[4] Riley E Brandt, Vladan Stevanović, David S Ginley, and Tonio Buonassisi, *Identifying defect-tolerant semiconductors with high minority-carrier lifetimes: beyond hybrid lead halide perovskites*, MRS Commun. **5** (June 2015), no. 2, 265–275 (en).

[5] John C de Mello, H Felix Wittmann, and Richard H Friend, *An improved experimental determination of external photoluminescence quantum efficiency*, Adv. Mater. **9** (March 1997), no. 3, 230–232.

[6] M Era, S Morimoto, T Tsutsui, and S Saito, *Organic-inorganic heterostructure electroluminescent device using a layered perovskite semiconductor (C6H5C2H4NH3)2PbI4*, Appl. Phys. Lett. **65** (August 1994), no. 6, 676–678 (en).

[7] Felix Fries and Sebastian Reineke, *Statistical treatment of photoluminescence quantum yield measurements*, Sci. Rep. **9** (October 2019), no. 1, 15638 (en).

[8] Thomas Geske, Sri Ganesh R Bade, Matt Worden, Xin Shan, Junqiang Li, and Zhibin Yu, *Organometal halide perovskites for next generation fully printed and flexible LEDs and displays*, Flexible and stretchable medical devices, February 2018, pp. 199–214.

[9] Martin A Green, Anita Ho-Baillie, and Henry J Snaith, *The emergence of perovskite solar cells*, Nat. Photonics **8** (July 2014), no. 7, 506–514 (en).

[10] N C Greenham, I D W Samuel, G R Hayes, R T Phillips, Y A R R Kessener, S C Moratti, A B Holmes, and R H Friend, *Measurement of absolute photoluminescence quantum efficiencies in conjugated polymers*, Chem. Phys. Lett. **241** (July 1995), no. 1-2, 89–96 (en).

[11] Yasser Hassan, Olivia J Ashton, Jong Hyun Park, Guangru Li, Nobuya Sakai, Bernard Wenger, Amir-Abbas Haghighirad, Nakita K Noel, Myoung Hoon Song, Bo Ram Lee, Richard H Friend, and Henry J Snaith, *Facile synthesis of stable and highly luminescent methylammonium lead halide nanocrystals for efficient light emitting devices*, J. Am. Chem. Soc. **141** (January 2019), no. 3, 1269–1279 (en).

[12] Beibei Jiang, James Iocozzia, Lei Zhao, Hefeng Zhang, Yeu-Wei Harn, Yihuang Chen, and Zhiqun Lin, *Barium titanate at the nanoscale: controlled synthesis and dielectric and ferroelectric properties*, Chem. Soc. Rev. **48** (February 2019), no. 4, 1194–1228 (en).

[13] Jun Kang and Lin-Wang Wang, *High defect tolerance in lead halide perovskite CsPbBr3*, J. Phys. Chem. Lett. **8** (January 2017), no. 2, 489–493 (en).

[14] Akihiro Kojima, Kenjiro Teshima, Yasuo Shirai, and Tsutomu Miyasaka, *Organometal halide perovskites as visible-light sensitizers for photovoltaic cells*, J. Am. Chem. Soc. **131** (May 2009), no. 17, 6050–6051 (en).

[15] Maksym V Kovalenko, Loredana Protesescu, and Maryna I Bodnarchuk, *Properties and potential optoelectronic applications of lead halide perovskite nanocrystals*, Science **358** (November 2017), no. 6364, 745–750 (en).

[16] Xiaoming Li, Ye Wu, Shengli Zhang, Bo Cai, Yu Gu, Jizhong Song, and Haibo Zeng, *CsPbX3Quantum dots for lighting and displays: Room-temperature synthesis, photoluminescence superiorities, underlying origins and white light-emitting diodes*, Adv. Funct. Mater. **26** (April 2016), no. 15, 2435–2445 (en).

[17] David B Mitzi, *Synthesis, structure, and properties of organic-inorganic perovskites and related materials*, Progress in inorganic chemistry, March 2007, pp. 1–121.

[18] M. Montalti, A. Credi, L. Prodi, and M.T. Gandolfi, *Handbook of photochemistry*, CRC Press, 2006.

[19] David P Nenon, Kimo Pressler, Jun Kang, Brent A Koscher, Jacob H Olshansky, Wojciech T Osowiecki, Matthew A Koc, Lin-Wang Wang, and A Paul Alivisatos, *Design principles for trap-free CsPbX3 nanocrystals: Enumerating and eliminating surface halide vacancies with softer lewis bases*, J. Am. Chem. Soc. **140** (December 2018), no. 50, 17760–17772 (en).

[20] Nakita K Noel, Severin N Habisreutinger, Bernard Wenger, Matthew T Klug, Maximilian T Hörantner, Michael B Johnston, Robin J Nicholas, David T Moore, and Henry J Snaith, *A low viscosity, low boiling point, clean solvent system for the rapid crystallisation of highly specular perovskite films*, Energy Environ. Sci. **10** (2017), no. 1, 145–152 (en).

[21] Nakita K Noel, Bernard Wenger, Severin N Habisreutinger, Jay B Patel, Timothy Crothers, Zhiping Wang, Robin J Nicholas, Michael B Johnston, Laura M Herz, and Henry J Snaith, *Highly crystalline methylammonium lead tribromide perovskite films for efficient photovoltaic devices*, ACS Energy Lett. **3** (June 2018), no. 6, 1233–1240 (en).

[22] Jong Hyun Park, Ah-Young Lee, Jae Choul Yu, Yun Seok Nam, Yonghoon Choi, Jongnam Park, and Myoung Hoon Song, *Surface ligand engineering for efficient perovskite nanocrystal-based light-emitting diodes* **11** (February 2019), no. 8, 8428–8435 (en).

[23] Loredana Protesescu, Sergii Yakunin, Maryna I Bodnarchuk, Franziska Krieg, Riccarda Caputo, Christopher H Hendon, Ruo Xi Yang, Aron Walsh, and Maksym V Kovalenko, *Nanocrystals of cesium lead halide perovskites (CsPbX, X = cl, br, and i): Novel optoelectronic materials showing bright emission with wide color gamut*, Nano Lett. **15** (June 2015), no. 6, 3692–3696 (en).

[24] Sara R Smock, Travis J Williams, and Richard L Brutchey, *Quantifying the thermodynamics of ligand binding to $CsPbBr_3$ quantum dots*, Angew. Chem. Int. Ed Engl. **57** (September 2018), no. 36, 11711–11715 (en).

[25] Constantinos C Stoumpos, Christos D Malliakas, and Mercouri G Kanatzidis, *Semiconducting tin and lead iodide perovskites with organic cations: phase transitions, high mobilities, and near-infrared photoluminescent properties*, Inorg. Chem. **52** (August 2013), no. 15, 9019–9038 (en).

[26] Dmitri V Talapin, Jong-Soo Lee, Maksym V Kovalenko, and Elena V Shevchenko, *Prospects of colloidal nanocrystals for electronic and optoelectronic applications*, Chem. Rev. **110** (January 2010), no. 1, 389–458 (en).

[27] Zhi-Kuang Tan, Reza Saberi Moghaddam, May Ling Lai, Pablo Docampo, Ruben Higler, Felix Deschler, Michael Price, Aditya Sadhanala, Luis M Pazos, Dan Credgington, Fabian Hanusch, Thomas Bein, Henry J Snaith, and Richard H Friend, *Bright light-emitting diodes based on organometal halide perovskite*, Nat. Nanotechnol. **9** (September 2014), no. 9, 687–692 (en).

[28] Feng Wang, Hui Yu, Haihua Xu, and Ni Zhao, *HPbI3: A new precursor compound for highly efficient solution-processed perovskite solar cells*, Adv. Funct. Mater. **25** (February 2015), no. 7, 1120–1126 (en).

[29] G Weber and F W J Teale, *Determination of the absolute quantum yield of fluorescent solutions*, Trans. Faraday Soc. **53** (1957), 646.

[30] Christian Wehrenfennig, Giles E Eperon, Michael B Johnston, Henry J Snaith, and Laura M Herz, *High charge carrier mobilities and lifetimes in organolead trihalide perovskites*, Adv. Mater. **26** (March 2014), no. 10, 1584–1589 (en).

[31] M K Wu, J R Ashburn, C J Torng, P H Hor, R L Meng, L Gao, Z J Huang, Y Q Wang, and C W Chu, *Superconductivity at 93 K in a new mixed-phase Yb-Ba-Cu-O compound system at ambient pressure*, Phys. Rev. Lett. **58** (March 1987), no. 9, 908–910 (en).

[32] Guichuan Xing, Nripan Mathews, Shuangyong Sun, Swee Sien Lim, Yeng Ming Lam, Michael Grätzel, Subodh Mhaisalkar, and Tze Chien Sum, *Long-range balanced electron- and hole-transport lengths in organic-inorganic CH3NH3PbI3*, Science **342** (October 2013), no. 6156, 344–347 (en).

[33] Yi Yu, Yingyi Tang, Bingfeng Wang, Kai Zhang, Jian-Xin Tang, and Yan-Qing Li, *Red perovskite light-emitting diodes: Recent advances and perspectives*, Laser Photon. Rev. (November 2022), 2200608 (en).